Opanasopit, P., Yokoyama, M., Watanabe, M., Kawano, K., Maitani, Y., Okano, T., 2004. Block copolymer design for camptothecin incorporation into polymeric micelles for passive tumor targeting. Pharm. Res. 21, 2003–2010.
Pan, D., Caruthers, S.D., Hu, G., Senpan, A., Scott, M.J., Gaffney, P.J., Wickline, S.A., Lanza, G.M., 2008. Ligand-directed nanobialys as theranostic agent for drug delivery and manganese-based magnetic resonance imaging of vascular targets. J. Am. Chem. Soc. 130, 9186–9187.
Rapoport, N., Gao, Z., Kennedy, A., 2007. Multifunctional nanoparticles for combining ultrasonic tumor imaging and targeted chemotherapy. J. Natl. Cancer Inst. 99, 1095–1106.
Rapoport, N.Y., Kennedy, A.M., Shea, J.E., Scaife, C.L., Nam, K.H., 2009a. Controlled and targeted tumor chemotherapy by ultrasound-activated nanoemulsions/microbubbles. J. Contr. Rel. 138, 268–276.
Rapoport, N.Y., Nam, K.H., Gao, Z., Kennedy, A., 2009b. Application of ultrasound for targeted nanotherapy of malignant tumors. Acoust. Phys. 55, 594–601.
Rapoport, N., Christensen, D.A., Kennedy, A.M., Nam, K.H., 2010a. Cavitation properties of block copolymer stabilized phase-shift nanoemulsions used as drug carriers. Ultrasound Med. Biol. 36, 419–429.
Rapoport, N., Kennedy, A.M., Shea, J.E., Scaife, C.L., Nam, K.H., 2010b. Ultrasonic nanotherapy of pancreatic cancer: lessons from ultrasound imaging. Mol. Pharm. 7, 22–31.
Rapoport, N., Nam, K.H., Gupta, R., Gao, Z., Mohan, P., Payne, A., Todd, N., Liu, X., Kim, T., Shea, J., Scaife, C., Parker, D.L., Jeong, E.K., Kennedy, A.M., 2011. Ultrasound-mediated tumor imaging and nanotherapy using drug loaded, block copolymer stabilized perfluorocarbon nanoemulsions. J. Contr. Rel. 153, 4–15.
Sanson, C., Diou, O., Thévenot, J., Ibarboure, E., Soum, A., Brûlet, A., Miraux, S., Thiaudière, E., Tan, S., Brisson, A., Dupuis, V., Sandre, O., Lecommandoux, S., 2011. Doxorubicin loaded magnetic polymersomes: theranostic nanocarriers for MR imaging and magneto-chemotherapy. ACS Nano 5, 1122–1140.
Schutt, E.G., Klein, D.H., Mattrey, R.M., Riess, J.G., 2003. Injectable microbubbles as contrast agents for diagnostic ultrasound imaging: the key role of perfluorochemicals. Angew. Chem. Int. Ed. Engl. 42, 3218–3235.
Shiraishi, K., Kawano, K., Minowa, T., Maitani, Y., Yokoyama, M., 2009. Preparation and in vivo imaging of PEG-poly(L-lysine)-based polymeric micelle MRI contrast agents. J. Contr. Rel. 136, 14–20.
Shiraishi, K., Kawano, K., Maitani, Y., Yokoyama, M., 2010. Synthesis of Poly(ethylene glycol)-b-poly(L-lysine) block copolymers having Gd-DOTA as MRI contrast agent and their polymeric micelle formation by polyion complexation. J. Contr. Rel. 148, 160–167.
Solans, C., Izquierdo, P., Nolla, J., Azemar, N., Garcia-Celma, M.J., 2005. Nano-emulsions. Curr. Opin. Colloid Interface Sci. 10, 102–110.
Tadros, T., Izuquierdo, P., Esquena, J., Solans, C., 2004. Formation and stability of nano-emulsions. Adv. Colloid Interface. Sci. 108–109, 303–318.
Tanigo, T., Takaoka, R., Tabata, Y., 2010. Sustained release of water-insoluble simvastatin from biodegradable hydrogel augments bone regeneration. J. Contr. Rel. 143, 201–206.
Unger, E.C., Porter, T., Culp, W., Labell, R., Matsunaga, T., Zutshi, R., 2004. Therapeutic applications of lipid-coated microbubbles. Adv. Drug Deliv. Rev. 56, 1291–1314.
Yamamoto, T., Yokoyama, M., Opanasopit, P., Hayama, A., Kawano, K., Maitani, Y., 2007. What are determining factors for stable drug incorporation into polymeric micelle carriers? Consideration on physical and chemical characters of the micelle inner core. J. Contr. Rel. 123, 11–18.
Yokoyama, M., 2005. Polymeric micelles for the targeting of hydrophobic drugs, In: Kwon, G.S. (Ed.), Drug and Pharmaceutical Sciences, Polymeric Drug Delivery Systems, 148. Taylor & Francis, Boca Raton, pp. 533–575.
Yokoyama, M., 2007. Polymeric micelles as nano-sized drug carrier systems. In: Domb, A.J., Tabata, Y., Kumar, M.N.V.R., Farber, S. (Eds.), Nanoparticles for Pharmaceutical Applications. American Scientific Publishers, Stevenson Ranch, pp. 63–72.
Yokoyama, M., Opanasopit, P., Maitani, Y., Kawano, K., Okano, T., 2004. Polymer design and incorporation method for polymeric micelle carrier system containing water-insoluble anti-cancer agent camptothecin. J. Drug Target. 12, 373–384.
Yuan, F., Dellian, M., Fukumura, D., Leunig, M., Berk, D.A., Torchilin, V.P., Jain, R.K., 1995. Vascular permeability in a human tumor xenograft: molecular size dependence and cutoff size. Cancer Res. 55, 3752–3756.
Watanabe, M., Kawano, K., Yokoyama, M., Opanasopit, P., Okano, T., Maitani, Y., 2006. Preparation of camptothecin-loaded polymeric micelles and evaluation of their incorporation and circulation stability. Int. J. Pharm. 308, 183–189.

International Journal of Cardiology 152 (2011) 202–206

Contents lists available at ScienceDirect

International Journal of Cardiology

journal homepage: www.elsevier.com/locate/ijcard

Enhancement of ultrasonic thrombus imaging using novel liposomal bubbles targeting activated platelet glycoprotein IIb/IIIa complex—*in vitro* and *in vivo* study

Kohsuke Hagisawa [a], Toshihiko Nishioka [b,*], Ryo Suzuki [c], Tomoko Takizawa [c], Kazuo Maruyama [c], Bonpei Takase [d], Masayuki Ishihara [d], Akira Kurita [d], Nobuo Yoshimoto [b], Fumitaka Ohsuzu [e], Makoto Kikuchi [a]

[a] Department of Medical Engineering, National Defense Medical College, 3-2 Namiki, Tokorozawa, Saitama 359-8513, Japan
[b] Division of Cardiology, Saitama Medical Center, Saitama Medical University, 1981 Kamoda, Kawagoe, Saitama 350-8550, Japan
[c] Department of Biopharmaceutics, School of Pharmaceutical Science, Teikyo University, 1091-1 Suwarashi, Sagamiko, Sagamihara, Kanagawa 229-0195, Japan
[d] Division of Biomedical Engineering, National Defense Medical College, 3-2 Namiki, Tokorozawa, Saitama 359-8513, Japan
[e] First Department of Internal Medicine, National Defense Medical College, 3-2 Namiki, Tokorozawa, Saitama 359-8513, Japan

ARTICLE INFO

Article history:
Received 12 February 2010
Received in revised form 19 June 2010
Accepted 4 July 2010
Available online 1 August 2010

Keywords:
Echocardiography
Thrombus
Imaging
Ultrasound
Liposome

ABSTRACT

Background: We developed perfluorocarbon gas-containing bubble liposomes (BL) with Arg-Gly-Asp (RGD) sequence-containing peptides, which bind to activated platelet glycoprotein IIb/IIIa complexes. The aim of this study was to examine the enhancing effects in ultrasonic thrombus imaging using these targeted BL *in vitro* and *in vivo*.

Methods: Liposomes composed of phosphatidylcholine and cholesterol were manufactured, and RGD peptide was attached by a covalent coupling reaction. Sonication was used to conjugate liposomes and perfluorocarbon gas, which formed targeted BL. *In vitro*, targeted BL were mixed with whole blood, which was allowed to coagulate while being shaken and rotated. *In vivo*, we administered targeted BL to 10 rabbits with acute thrombotic occlusions in the ilio-femoral artery. Thrombi were imaged using a 7.5–9 MHz linear transducer and a conventional ultrasound machine, and by scanning electron microscopy. Ultrasound images were digitized, and mean pixel gray-scale level (black = 0, white = 255) was measured.

Results: *In vitro*, mean pixel gray-scale level of the thrombi in targeted BL group was significantly higher than in control and non-targeted BL groups (93 ± 26 vs. 58 ± 16, 48 ± 9, $p = 0.002$, $n = 10$). Scanning electron microscopy revealed large amounts of targeted BL attached to the thrombi. *In vivo*, mean pixel gray-scale level of the thrombi with targeted BL was significantly higher (33.2 ± 6.4 vs. 24.8 ± 8.5, $p = 0.0051$, $n = 10$) than that before targeted BL administration.

Conclusions: Perfluorocarbon gas-containing BL with RGD peptide represent a novel echo contrast agent, which can markedly enhance ultrasonic thrombus imaging *in vitro* and *in vivo*, and may be useful for noninvasively diagnosing acute thrombotic vessel occlusion.

1. Introduction

Echocardiographic diagnosis of vascular or intracardiac thrombi is sometimes challenging, even using state-of-the-art ultrasound systems and comercially available ultrasound contrast agents [1,2]. Intravascular ultrasound imaging provides more detailed pictures of thrombi due to its higher frequency; however, thrombi within the vessel lumen can often be mistaken for soft plaques, unless they are distinguished from soft plaques by mobility, lobular edges and movement away from the vessel wall during the cardiac cycle [3]. Therefore, it is essential to improve the diagnostic accuracy of echocardiography for detecting thrombi *in vivo*.

Recently, using emerging molecular imaging techniques, several types of novel thrombus-targeting ultrasound contrast agents have been developed and examined for use in the diagnosis of thrombi *in vitro* and in animal models [4–10]. These ultrasound contrast agents are lipid-encapsulated perfluorocarbon gas or nongaseous liposomes, and antibodies or peptides are used as specific ligands to fibrin or platelets. However, these agents are not commercially available.

We have developed novel polyethylene glycol-modified liposomal bubbles (bubble liposomes, BL) containing perfluoropropane gas, which can be used as an ultrasound contrast agent [11–13]. We attached targeted ligands for activated platelets to these BL. We used Arg-Gly-Asp (RGD) sequence-containing peptides, which bind to the

* Corresponding author. Tel.: +81 49 228 3587; fax: +81 49 226 5274.
E-mail address: nishioka@saitama-med.ac.jp (T. Nishioka).

0167-5273/$ – see front matter © 2010 Elsevier Ireland Ltd. All rights reserved.
doi:10.1016/j.ijcard.2010.07.016

fibrinogen receptor on the activated platelet membrane glycoprotein IIb/IIIa complex [14–17]. We hypothesized that the activated thrombus-targeting BL would enhance fresh thrombus visualization by conventional transcutaneous ultrasound and may enable diagnosis of acute thrombotic vessel occlusion. The aim of this study was to examine the enhancing effects on ultrasonic imaging of fresh thrombi using these BL *in vitro* and *in vivo*.

2. Materials and methods

2.1. Preparation of thrombus-targeting BL

The lipid-based shell of the perfluorocarbon gas-containing BL was composed of 12.6 mg of 1,2-distearoyl-sn-glycero-phosphatidylcholine (DSPC) (NOF Corp., Tokyo, Japan), 5.1 mg of 1,2-distearoyl-sn-glycero-3-phosphatidyl-ethanolamine-m-poly-ethyleneglycol 2000 maleimide (DSPE-PEG-Mal-2000; Avanti, Alabaster, AL) and 3.0 mg of cholesterol (Sigma-Aldrich Japan, Tokyo, Japan). Liposomes were prepared by reverse phase evaporation [16]. Briefly, a mixture of all reagents was dissolved in 2.0 ml of chloroform and mixed with the same amount of di-isopropyl ether and normal saline. The mixture was sonicated using a probe-type 19.5-kHz ultrasound at 550 W (XL-2020 Sonicator, Misonix, Inc., Farmingdale, NY) and then evaporated at 65 °C using a rotary evaporating system (Tokyo Rika, Tokyo, Japan). After the chemical solvent was completely removed, the size of liposomes was adjusted to be less than 0.2 μm using extruding equipment and a membrane filter (Northern Lipids, Inc., Vancouver, Canada) with sizing filters. To the liposome liquid, 1 mg of linear octapeptide with an amino acid sequence of cysteine–glycine–glycine–glycine–arginine–glycine–aspartic acid–phenyl-alanine (CGGGRGDF) (Operon Biotechnologies, Tokyo, Japan) was added [14,17] and allowed to conjugate to the maleimide on the liposomal surface via thio-ether covalent coupling at room temperature for 2 h. Gel filtration was then used to remove unreacted peptide fragments. Lipid concentration was measured with the Wako Phospholipid C test (Wako Pure Chemical Industries, Osaka, Japan) and the RGD-liposomes were diluted to a final concentration of 20 mg/ml. The RGD-liposomes were sealed in a 5-ml vial and air was exchanged with perfluoropropane gas (Takachiho Chemical Ind. Co., Ltd., Tokyo, Japan), followed by 20-kHz ultrasound treatment using a bath-type sonicating system (Branson model 3510, Emerson, CT) for 5 min to generate RGD-BL [11,12]. Sterilized filtration (0.45 μm) was then performed to remove expanded and oversized BL. Non-targeted BL were also prepared in the same manner, except without the addition of RGD peptides. The diameter of each BL was determined by dynamic laser light-scattering measurements using the ELS-800 particle analyzer (Otsuka Electronics, Osaka, Japan).

2.2. In vitro thrombus imaging

In total, 30 thrombi were used in this *in vitro* study. For preparation of each thrombus, 9 ml of whole blood was collected in a test tube from a healthy volunteer, placed on a seesaw-type shaker and allowed to coagulate at room temperature while being shaken and rotated at a speed of 60 rpm for 1 h. Ten thrombi served as controls, non-targeted BL were added to 10 thrombi and targeted BL were added to the remaining 10 thrombi. Targeted BL or non-targeted BL (100 μl, 20 mg/ml lipid concentration) were added to the test tube after 10 min. The formed thrombi were washed with normal saline, cut into small pieces and placed in a latex tube filled with degassed water. Thrombi were imaged using a 7.5-MHz linear transducer with a conventional ultrasound machine (SONOS2000, Philips Medical Systems, Potomac, MD) (frame rate, 40–50/s; mechanical index, 0.4) in a bath filled with degassed water. As a control, 10 thrombi prepared without BL were also imaged at the same gain setting and ultrasound intensity. For quantitative analysis, the mean video intensity level of whole thrombi was measured on a 256 gray-scale level (black = 0, white = 255) using NIH image software [18].

2.3. Scanning electron microscopic observation of thrombi

Thrombi were prepared as described for the *in vitro* thrombus imaging study. Thrombi with targeted BL, non-targeted BL or saline were fixed in 2% glutaraldehyde in normal saline and dehydrated in a graded ethanol series. Thrombi were further cut and divided into smaller pieces in order to observe the inside as well as the surface. This was followed by critical-point drying and gold sputtering (JEOL JFC-1100, Nippon Denshi, Tokyo, Japan). Specimens were then examined with a conventional scanning electron microscope (JOEL Carry Scope, Nippon Denshi, Tokyo, Japan) at an acceleration voltage of 5 to 15 kV [19].

2.4. Acute thrombotic occlusion model of rabbit ilio-femoral artery

This study followed the American Physiological Society Guidelines for Animal Research, which conform to the "Position of the American Heart Association on Research Animal Use" adopted by the AHA in November 1984. A total of 20 New Zealand white rabbits were used; 10 each for the targeted BL study and the non-targeted BL study. Each rabbit was anesthetized using 50 mg of ketamine and 20 mg of xylazine. Anesthesia was maintained with pentbarbitrate (15 mg/kg). A 5-Fr sheath was inserted into the right carotid artery, a balloon catheter was advanced to the ilio-femoral artery, and the intima was injured by balloon inflation. Afterwards, the balloon catheter was pulled back, a 0.014-inch guide wire was positioned at the injury site, and electrical stimulation (from a 3-V battery) was applied between the guide wire and skin electrode [20,21]. After 30 min, the artery was thrombotically occluded and arterial occlusion was confirmed by angiography.

2.5. In vivo thrombus imaging

The thrombus was imaged in a longitudinal axis view using a 9-MHz linear transducer and a conventional ultrasound machine (UF-750XT, Fukuda Denshi, Ltd., Tokyo, Japan) (frame rate, 24–30/s; mechanical index, 0.3). Manipulating the transducer just above the angiographic vessel occlusion site, the ultrasonic occlusion site was identified as an abrupt interruption of echo-Doppler signal within the vessel. The region of interest was then defined as the area between the near and far vessel walls without a Doppler signal, according to the consensus of two cardiologists (K.H. and T.N.). To maintain the same view, the ultrasound transducer was fixed with a hand-free stabilizer. The ultrasound thrombus images were continuously recorded from just before to 10 min after the bolus injection of targeted BL (1 ml, 20 mg/ml lipid concentration) through the ear vein in 10 rabbits. After the experiment, the video intensity of the thrombus was measured using NIH image, as described for the *in vitro* study. As controls, the video intensity of the thrombi was measured before and after injection of 1 ml (20 mg/ml lipid concentration) of non-targeted (without RGD peptide) BL in another 10 rabbits.

2.6. Statistical analyses

Results are given as means ± 1 standard deviation. As video intensity levels of the thrombi were not considered to be normally distributed, non-parametric tests were used to compare data. For the *in vitro* study, thrombus echo intensity was compared and analyzed using the Kruskal–Wallis test followed by a post-hoc Bonferroni test. For the *in vivo* study, thrombus echo intensity before and after BL administration was compared by the Wilcoxon-signed rank sum test. A p value <0.05 was considered statistically significant.

3. Results

3.1. In vitro thrombus imaging

Ultrasonic images of thrombi were apparently enhanced when compared to the control and non-targeted BL groups (Fig. 1A). The mean pixel gray-scale levels of the control and non-targeted BL thrombi were not significantly different. However, the mean pixel gray-scale level of the thrombi in the targeted BL group was significantly higher than those in the control and non-targeted BL thrombus groups (93 ± 26 vs. 58 ± 16, 48 ± 9, $p = 0.0001$, $n = 10$) (Fig. 1B). Enhancement of ultrasonic thrombus imaging in the targeted BL group lasted at least 15 min, at which point observation was discontinued. BL diameter was 0.185 ± 0.044 μm.

3.2. Scanning electron microscopic observation of thrombi

Large amounts of targeted BL were attached to the fibrin nets and platelets on the surface of thrombi, as well as in the deep inner portions of thrombi (Fig. 2C). In contrast, no BL were attached to the thrombi in the non-targeted BL and control groups (Fig. 2A and B). Targeted BL were smaller than the fibrin mesh (<0.2 μm) in all observed fields.

3.3. In vivo thrombus imaging

The rabbit ilio-femoral arterial thrombus was clearly visualized using a conventional ultrasound system with the targeted BL (Fig. 3A). After targeted BL injection, the mean pixel gray-scale level of the thrombus rapidly peaked (within 1 min) and then gradually decreased; however, it did not return to baseline levels, even after 10 min (Fig. 4). Targeted BL significantly increased the mean pixel gray-scale level of the thrombus at 1 min when compared to that before targeted BL administration (33.2 ± 6.4 vs. 24.8 ± 8.5, $p = 0.0051$, $n = 10$). After non-targeted BL injection, blood echo intensity around the thrombus was increased; however, no significant increases were observed in the

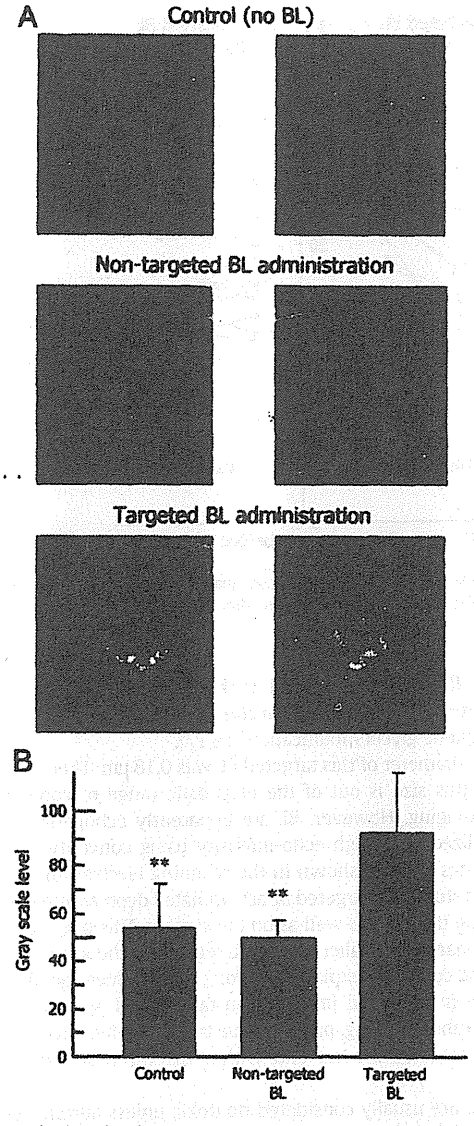

Fig. 1. Ultrasonic thrombus imaging is apparently enhanced by targeted BL *in vitro* when compared to control and non-targeted BL (A). Video intensity levels of the thrombi in the targeted BL group were significantly higher than in the control and non-targeted BL groups (B). BL: bubble liposomes.

mean pixel gray-scale level of the thrombus at 1 min (25.5 ± 4.8 vs. 26.4 ± 5.3, $p = 0.3329$, $n = 10$) (Fig. 3B and C).

4. Discussion

In our *in vitro* and *in vivo* studies, we confirmed that ultrasound imaging of thrombi is markedly enhanced by targeted BL, even via intravenous administration using a conventional diagnostic ultrasound machine. This is also the first study to show the feasibility of perfluorocarbon gas-containing liposomes, rather than a phospholipid mono-layer, as a targeted ultrasound contrast agent, in addition to a carrier for gene delivery [11–13].

In clinical settings, various ultrasound contrast agents with lipid-based or non-lipid-based shells are commercially available for diagnostic use. These agents are prepared to enhance blood flow or tissue perfusion. Some of these agents are capable of passively imaging inflammation using the inherent chemical properties of the shell components [22]. However, they have no specific ligands on their surface for actively targeting pathophysiological molecules.

Lanza et al. first reported a fibrin-targeting ultrasonic contrast agent. They used lipid-encapsulated, nongaseous perfluorocarbon emulsion and an antifibrin monoclonal antibody as a targeting ligand, incorporating avidin-biotin triphasic interaction steps to demonstrate excellent thrombus enhancement [4]. However, this technique has limited applications in humans due to the complexity of targeting interactions and immunogenicity of avidin [23]. Unger et al. developed thrombus-targeting perfluorocarbon gas-containing microbubbles with lipid mono-layer shells incorporating small peptides as ligands for activated platelets [5–7]. This agent was able to enhance ultrasonic thrombus imaging both *in vitro* and *in vivo* during continuous intravenous infusion. Demos and Hamilton reported thrombus-targeting nongaseous echogenic immuno-liposomes, which enhanced ultrasonic imaging of both intravascular and intracardiac thrombi [8,9]. In this study, anti-fibrinogen antibody was used as the targeting ligand, which may cause systemic adverse effects due to secondary immunoreactions. Alonso et al. developed abciximab, an antibody fragment specific for the glycoprotein IIb/IIIa receptor, bearing immunobubbles with phospholipid mono-layer shells. These immunobubbles improved visualization of human clots both *in vitro* and in an *in vivo* model of acute arterial thrombotic occlusion [10].

Targeted BL shows some advantages over these previously reported thrombus-targeting ultrasound contrast agents [4–10]. We used liposomes as a basic structure, as a lipid bi-layer shell increases the stability of BL and works as a barrier against gas diffusion [12], and the liposomal surface can be modified for the conjugation of various targeted ligands, as well as for achieving longer circulation times. Polyethylene glycol was attached to the surface lipid layer in order to

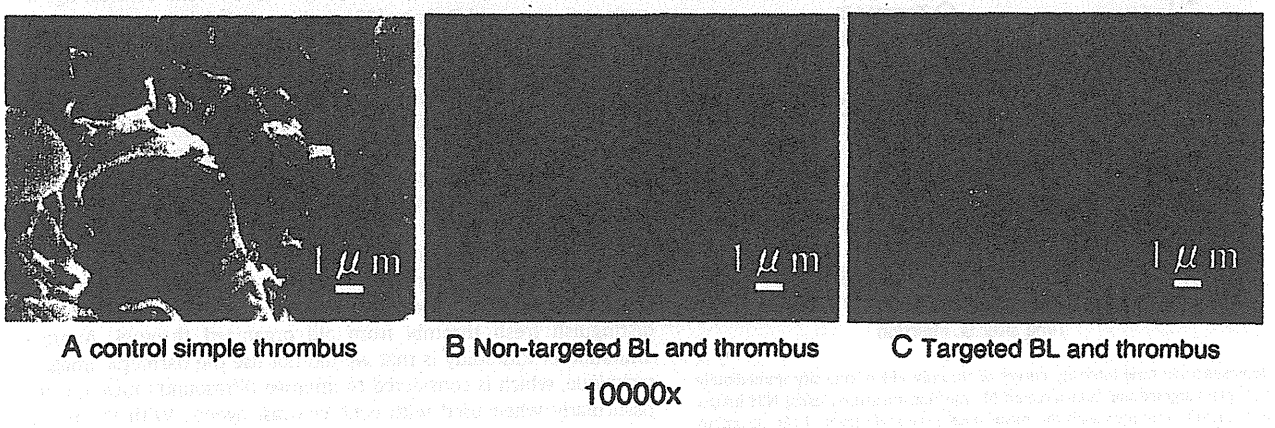

Fig. 2. Scanning electron microscopy revealed large amounts of BL attached to the thrombi in the targeted BL group (C), which were not observed in the non-targeted BL (B) and control groups (A). BL: bubble liposomes.

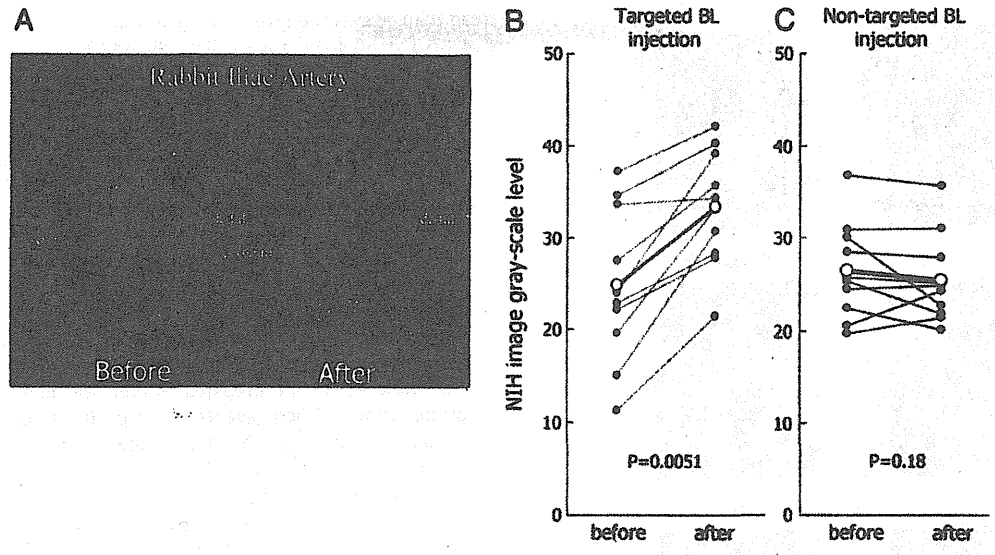

Fig. 3. Ultrasound image of *in vivo* thrombi is significantly enhanced after administration of targeted BL via an ear vein. (A) NIH image quantitative analysis shows significant increases on *in vivo* thrombus echo intensity by intravenous administration of targeted BL; (B) however, similar changes are not seen after administration of non-targeted BL (C). BL: bubble liposomes.

increase hydrophilicity, thereby offering a stealth effect with respect to reticulo-endothelial capture and allowing longer circulation times [24,25]. Moreover, a BL size of less than a micron (nano-size) permits deeper penetration into thrombi.

The targets of ultrasonic thrombus imaging have been fibrin [4,8,9] or activated platelets [5–7,10]. Fibrin is typically present in all types of thrombi (arterial and venous, acute and chronic). In contrast, activated platelets are found in fresh thrombi in cases of acute coronary syndrome and stroke. The RGD sequence-containing peptide is a ligand for the activated platelet membrane glycoprotein IIb/IIIa complex. The RGD peptide is chemically stable and easily conjugated to the lipid surface layer, as it is composed of a small number of amino acids and binds strongly to phospholipids via a thio-ether bond without the need for complex chemical synthesis [14,15]. In contrast to antibodies, peptides are generally smaller in size and simpler in structure, resulting in less immunoreactivity [26,27]. Among the various types of RGD peptides, we used an octapeptide (CGGGRGDF) in this study. The initial C of this peptide was used for coupling and GGG served as an "arm" to distance the active RGD binding site from thiol-coupling to maleimide on the liposomal surface [17]. Moreover, this peptide has been reported to be a potent inhibitor of platelet agglutination through the glycoprotein IIb/IIIa receptor, and to be uniquely sensitive to the activation state of this receptor, even after incorporation into liposomes with polyethylene glycol modification [14,17].

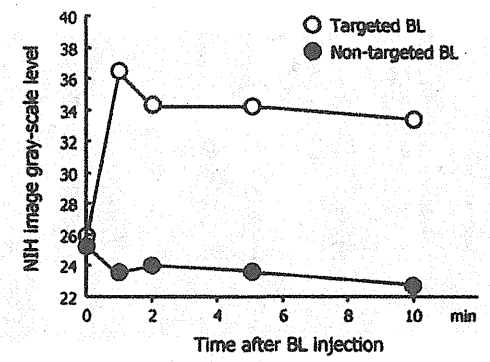

Fig. 4. Representative time-intensity curves of thrombi video intensity immediately before and after targeted and non-targeted BL injection measured using NIH image. Targeted BL significantly increased the mean pixel gray-scale level of the thrombus from 1 to 10 min after injection; however, no significant increases were observed after non-targeted BL injection. BL: bubble liposomes.

The mean diameter of this targeted BL was 0.18 μm. Theoretically, a single BL of this size is out of the diagnostic range of conventional ultrasound imaging. However, BL are apparently echogenic and are clearly visualized with high echo-intensity using conventional ultrasound machines [11]. As shown in the scanning electron microscopic section of this study, the targeted BL accumulated deep within the inner portions of the thrombi, as well as on the surface. This may have been due to the apparently smaller size of BL relative to the space between fibrin nets, and could also explain the strong enhancement on ultrasonic imaging both *in vitro* and *in vivo*. Non-targeted BL were unable to enhance thrombus imaging, probably due to the insufficient amount of BL passively retained around and within the thrombi required for echogenicity.

Liposomes are usually considered nontoxic unless administered at very high doses [28]. Liposomal drugs are already commercially available and are safely used in humans [29–31]. Polyethylene glycol is also considered nontoxic and is excreted unmetabolized in the urine [32]. The RGD peptide is an octapeptide and is considered to be non-toxic and non-immunogenic [26,27]. Perfluoropropane is an inert gas, used as a constituent of commercially available echo contrast agents such as Optison and Definity [33], and is exhaled from the lungs [34]. Therefore, this echo contrast agent is generally considered nontoxic, although safety in humans remains to be demonstrated. Other potential barriers for clinical use are related to the specificity of the RGD peptide. This ligand is highly specific to activated platelet glycoprotein IIb/IIIa receptor [14,17]. However, the specificity is limited and this ligand may also bind to sites of angiogenesis, inflammation, osteoporosis and cancer [35]. In contrast, the relatively high specificity of this ligand to activated platelets may prevent the attachment of the targeted BL to organized chronic thrombi, although this hypothesis was not examined in the present experiment. Therefore, this agent may only enhance fresh thrombi on imaging and may provide a unique opportunity to distinguish fresh thrombi from old organized thrombi. Another limitation of this study is that we did not use the harmonic imaging technique, which is considered to improve ultrasound image quality, particularly when used with echo contrast agents. With the use of harmonic imaging, more distinct enhancement of thrombi can be expected in larger animals or humans.

In conclusion, perfluorocarbon gas-containing liposomal bubbles with RGD peptides are a novel echo contrast agent that can markedly enhance fresh thrombi on ultrasonic imaging *in vitro* and *in vivo*, and may be useful for noninvasive diagnosis of acute thrombotic vessel occlusion.

Acknowledgements

This study was supported in part by a Grant-in-Aid for Scientific Research (B) (16300176) from the Japan Society for the Promotion of Science and a Japan Heart Foundation Research Grant.

The authors of this manuscript have certified that they comply with the Principles of Ethical Publishing in the International Journal of Cardiology [36].

References

[1] Masses, tumors, and source of embolus. In: Feigenbaum H, Armstrong WF, Ryan T, editors. Feigenbaum's echocardiography. 6th ed. Philadelphia, PA: Lippincott Williams & Wilkins; 2005. p. 701–34.
[2] Rose SC, Zwiebel WJ, Murdock LE, et al. Insensitivity of color Doppler flow imaging for detection of acute calf deep venous thrombosis in asymptomatic postoperative patients. J Vasc Interv Radiol 1993;4:111–7.
[3] Popma JJ. Coronary arteriography and intravascular imaging. In: Libby P, Bonow RO, Mann DL, Zipes DP, editors. Braunwald's heart disease: a textbook of cardiovascular medicine. 8th ed. Philadelphia, PA: Saunders Elsevier; 2008. p. 495–6.
[4] Lanza GM, Wallace KD, Scott MJ, et al. A novel site-targeted ultrasonic contrast agent with broad biomedical application. Circulation 1996;94:3334–40.
[5] Unger EC, McCreery TP, Sweitzer RH, Shen D, Wu G. In vitro studies of a new thrombus-specific ultrasound contrast agent. Am J Cardiol 1998;81:58G–61G.
[6] Wu Y, Unger EC, McCreery TP, et al. Binding and lysing of blood clots using MRX-408. Invest Radiol 1998;33:880–5.
[7] Takeuchi M, Ogunyankin K, Pandian NG, et al. Enhanced visualization of intravascular and left atrial appendage thrombus with the use of a thrombus-targeting ultrasonographic contrast agent (MRX-408A1): in vivo experimental echocardiographic studies. J Am Soc Echocardiogr 1999;12:1015–21.
[8] Demos SM, Alkan-Onyuksel H, Kane BJ, et al. In vivo targeting of acoustically reflective liposomes for intravascular and transvascular ultrasonic enhancement. J Am Coll Cardiol 1999;33:867–75.
[9] Hamilton A, Huang SL, Warnick D, et al. Left ventricular thrombus enhancement after intravenous injection of echogenic immunoliposomes: studies in a new experimental model. Circulation 2002;105:2772–8.
[10] Alonso A, Della Martina A, Stroick M, et al. Molecular imaging of human thrombus with novel abciximab immunobubbles and ultrasound. Stroke 2007;38:1508–14.
[11] Suzuki R, Takizawa T, Negishi Y, et al. Gene delivery by combination of novel liposomal bubbles with perfluoropropane and ultrasound. J Control Release 2007;117:130–6.
[12] Suzuki R, Takizawa T, Negishi Y, et al. Tumor specific ultrasound enhanced gene transfer in vivo with novel liposomal bubbles. J Control Release 2008;125:137–44.
[13] Suzuki R, Takizawa T, Negishi Y, Utoguchi N, Maruyama K. Effective gene delivery with liposomal bubbles and ultrasound as novel non-viral system. J Drug Target 2007;15:531–7.
[14] Gyongyossy-Issa MIC, Muller W, Devine DV. The covalent coupling of Arg-Gly-Asp-containing peptides to liposomes: purification and biochemical function of the lipopeptide. Arch Biochem Biophys 1998;353:101–8.
[15] Nishiya T, Sloan S. Interaction of RGD liposomes with platelets. Biochem Biophys Res Commun 1996;224:242–5.
[16] Szoka Jr F, Papahadjopolus D. Procedure for preparation of liposomes with large internal aqueous space and high capture by reverse-phase evaporation. Proc Natl Sci U S A 1978;75:4194–8.
[17] Beer JH, Springer KT, Coller BS. Immobilized Arg-Gly-Asp (RGD) peptides of varying lengths as structural probes of the platelet glycoprotein IIb/IIIa receptor. Blood 1992;79:117–28.
[18] NIH image home page. http://rsb.info.nih.gov/nih-image/ Accessed January 29, 2010.
[19] Glauert AM, Lewis PR. Biological specimen preparation for transmission electron microscopy. In: Glauert AM, editor. Practical methods in electron microscopy Volume 17. London, UK: Portland Press; 1998.
[20] Steffen W, Fishbein MC, Luo H, et al. High intensity, low frequency catheter-delivered ultrasound dissolution of occlusive coronary artery thrombi: an in vitro and in vivo study. J Am Coll Cardiol 1994;24:1571–9.
[21] Nishioka T, Luo H, Fishbein MC, et al. Dissolution of thrombotic arterial occlusion by high intensity, low frequency ultrasound and dodecafluoropentane emulsion: an in vitro and in vivo study. J Am Coll Cardiol 1997;30:561–8.
[22] Lindner JR. Microbubbles in medical imaging: current applications and future directions. Nature Rev Drug Discov 2004;3:527–32.
[23] Lanza GM, Wickline SA. Targeted ultrasonic contrast agents for molecular imaging and therapy. Curr Probl Cardiol 2003;28:625–53.
[24] Klibanov AL, Maruyama K, Torchilin VP, Huang L. Amphipathic polyethyleneglycols effectively prolong the circulation time of liposomes. FEBS Lett 1990;268:235–7.
[25] Maruyama K, Yuda T, Okamoto A, Kojima S, Suginaka A, Iwatsuru M. Prolonged circulation time in vivo of large unilamellar liposomes composed of distearoyl phosphatidylcholine and cholesterol containing amphipathic poly(ethylene glycol). Biochim Biophys Acta 1992;1128:44–9.
[26] Lee TY, Lin CT, Kuo SY, Chang DK, Wu HC. Peptide-mediated targeting to tumor blood vessels of lung cancer for drug delivery. Cancer Res 2007;67:10958–65.
[27] Chang DK, Lin CT, Wu CH, Wu HC. A novel peptide enhances therapeutic efficacy of liposomal anticancer drugs in mice models of human lung cancer. PLoS ONE 2009;4:e4171.
[28] Storm G, Oussoren C, Peelers PAM, Barenholz Y. Tolerability of liposomes *in vivo*. In: Gregoriadis G, editor. Liposome technology. Boca Raton, FL: CRC Press, Inc.; 1993. p. 345–83.
[29] Davidson RN, Croft SL, Scott A, Maini M, Moody AH, Bryceson AD. Liposomal amphotericin B in drug-resistant visceral leishmaniasis. Lancet 1991;337:1061–2.
[30] Guaglianone P, Chan K, DelaFlor-Weiss E, et al. Phase I and pharmacologic study of liposomal daunorubicin (DaunoXome). Invest New Drugs 1994;12:103–10.
[31] Gabizon A, Peretz T, Sulkes A, et al. Systemic administration of doxorubicin-containing liposomes in cancer patients: a phase I study. Eur J Cancer Clin Oncol 1989;25:1795–803.
[32] Carpenter CP, Woodside MD, Kinkead ER, King JM, Sullivan LJ. Response of dogs to repeated intravenous injection of polyethylene glycol 4000 with notes on excretion and sensitization. Toxicol Appl Pharmacol 1971;18:35–40.
[33] Wei K, Mulvagh SL, Carson L, et al. The safety of Definity and Optison for ultrasound image enhancement: a retrospective analysis of 78, 383 administered contrast doses. J Am Soc Echocardiogr 2008;11:1202–6.
[34] Hutter JC, Luu HM, Mehlhaff PM, Killam AL, Dittrich HC. Physiologically based pharmacokinetic model for fluorocarbon elimination after the administration of an octafluoropropane-albumin microsphere sonographic contrast agent. J Ultrasound Med 1999;18:1–11.
[35] Meyer A, Auernheimer J, Modlinger A, Kessler H. Targeting RGD recognizing integrins: drug development, biomaterial research, tumor imaging and targeting. Curr Pharm Des 2006;12:2723–47.
[36] Coats AJ. Ethical authorship and publishing. Int J Cardiol 2009;131:149–50.

Journal of Controlled Release 156 (2011) 355–363

Contents lists available at ScienceDirect

Journal of Controlled Release

journal homepage: www.elsevier.com/locate/jconrel

Involvement of activated transcriptional process in efficient gene transfection using unmodified and mannose-modified bubble lipoplexes with ultrasound exposure

Keita Un [a,b], Shigeru Kawakami [a,*], Yuriko Higuchi [c], Ryo Suzuki [d], Kazuo Maruyama [d], Fumiyoshi Yamashita [a], Mitsuru Hashida [a,e,*]

[a] Department of Drug Delivery Research, Graduate School of Pharmaceutical Sciences, Kyoto University, 46-29 Yoshida-Shimoadachi-cho, Sakyo-ku, Kyoto 606-8501, Japan
[b] The Japan Society for the Promotion of Science (JSPS), Chiyoda-ku, Tokyo 102-8471, Japan
[c] Institute for Innovative NanoBio Drug Discovery and Development, Graduate School of Pharmaceutical Sciences, Kyoto University, 46-29 Yoshida-Shimoadachi-cho, Sakyo-ku, Kyoto 606-8501, Japan
[d] Department of Biopharmaceutics, School of Pharmaceutical Sciences, Teikyo University, 1091-1 Suwarashi, Midori-ku, Sagamihara, Kanagawa 252-5195, Japan
[e] Institute for Integrated Cell-Material Sciences (iCeMS), Kyoto University, Yoshida-Ushinomiya-cho, Sakyo-ku, Kyoto 606-8302, Japan

ARTICLE INFO

Article history:
Received 6 May 2011
Accepted 27 June 2011
Available online 3 July 2011

Keywords:
Gene transfection
Bubble lipoplex
Ultrasound
Transcription factor
Inflammatory response

ABSTRACT

Recently, our group developed ultrasound (US)-responsive and mannose-modified gene carriers (Man-PEG_{2000} bubble lipoplexes), and successfully obtained a high level of gene expression in mannose receptor-expressing cells following gene transfection using Man-PEG_{2000} bubble lipoplexes and US exposure. We also reported that large amounts of plasmid DNA (pDNA) were transferred into the cytoplasm of the targeted cells in the gene transfection using this method. In the present study, we investigated the involvement of transcriptional processes on enhanced gene expression obtained by unmodified and Man-PEG_{2000} bubble lipoplexes with US exposure. The transcriptional process related to activator protein-1 (AP-1) and nuclear factor-κB (NFκB) was activated by US exposure, and was founded to be involved in enhanced gene expression obtained by gene transfection using unmodified and Man-PEG_{2000} bubble lipoplexes with US exposure. On the other hand, activation of AP-1 and NFκB pathways followed by US exposure was hardly involved in the inflammatory responses in the gene transfection using this method. These findings suggest that activation of AP-1 and NFκB followed by US exposure is involved in the enhanced gene expression using unmodified and Man-PEG_{2000} bubble lipoplexes with US exposure, and the selection of pDNAs activated by US exposure is important in this gene transfection method.

1. Introduction

Various obstacles are associated with in vivo gene transfection, including the control of in vivo distribution of nucleic acids, the improvement of intracellular/intranuclear transport of nucleic acids, and the activation of transcriptional/translational processes directly involved in the gene expression [1,2]. Viral and non-viral carriers have been studied as valuable gene carriers for in vivo gene transfection [3–6], with both possessing advantages and disadvantages relating to safety, productivity and gene expressing efficiency. Hama and Harashima et al. have reported that the high gene expression efficiency in gene transfection using viral carrier is influenced by the high transcriptional and translational efficiency following intranuclear transport of pDNA [7,8]. Therefore, the transcriptional/translational processes associated with gene transfection of non-viral carriers are potentially controlled by improved gene expression efficiency.

Gene transfection methods using physical stimulation, such as electroporation method [9], hydrodynamic injection [10,11], tissue pressure-mediated method [12] and sonoporation method [13], enable to obtain high-level gene expression. Gene expression has also been reported to be enhanced by intracytoplasmic transfer of pDNA as a result of using these methods [14–16]. Recently, our group developed US-responsive and/or mannose-modified gene carriers (unmodified and Man-PEG_{2000} bubble lipoplexes), and reported that high level gene expression can be selectively obtained in mannose receptor-expressing cells following intravenous administration of Man-PEG_{2000} bubble lipoplexes and US exposure, both in vitro and in vivo [17,18]. Furthermore, we have reported that large amounts of pDNA are transferred into the cytoplasm of targeted cells in the gene transfection using unmodified and Man-PEG_{2000} bubble lipoplexes with optimized US exposure under both in vitro and in vivo conditions [19].

Various types of physical stimulations, such as electric pulse, physical pressure, radiation and US exposure, can activate the transcriptional process involved in the AP-1-mediated and NFκB-

* Corresponding authors. Tel.: +81 75 753 4545; fax: +81 75 753 4575.
E-mail addresses: kawakami@pharm.kyoto-u.ac.jp (S. Kawakami), hashidam@pharm.kyoto-u.ac.jp (M. Hashida).

0168-3659/$ – see front matter © 2011 Elsevier B.V. All rights reserved.
doi:10.1016/j.jconrel.2011.06.040

mediated pathways [20–26]. It has been reported that this activation of transcription followed by physical stimulation partly contributes to the high gene expression observed when using the hydrodynamics and physical pressure-mediated methods [21,22,27]. However, there are few reports that the transcriptional process is activated by US exposure in vivo. Moreover, there is little information that the transcriptional activation followed by US exposure involves in the enhanced gene expression by in vitro and in vivo gene transfection using sonoporation method.

Our present study investigated the involvement of transcriptional processes in enhanced gene expression obtained by transfection using unmodified and Man-PEG_{2000} bubble lipoplexes with US exposure. We examined the gene transfection efficiency obtained by US-mediated gene transfection using pDNAs controlled by various transcription factors including AP-1, NFκB, cyclic adenosine 3′,5′-monophosphate response element (CRE) and serum response element (SRE), in RAW264.7 cell lines, primary mouse cultured macrophages, and mice. Then, we evaluated the gene expression and intranuclear transport of transcription factors, such as AP-1 [28] and NFκB [29,30], followed by gene transfection using unmodified and Man-PEG_{2000} bubble lipoplexes with US exposure, both in vitro and in vivo. Finally, the involvement of activated transcription on inflammatory cytokine production was also examined, since activation of specific transcriptional factors might contribute to the inflammatory responses [31,32].

2. Materials and methods

2.1. Materials

1,2-Distearoyl-*sn*-glycero-3-trimethylammoniumpropane (DSTAP), 1,2-distearoyl-*sn*-glycero-3-phosphocholine (DSPC) and 1,2-distearoyl-*sn*-glycero-3-phosphoethanolamine-N-[amino (polyethylene glycol)-2000] (NH_2-PEG_{2000}-DSPE) were purchased from Avanti Polar Lipids (Alabaster, AL, USA), Sigma-Aldrich (St. Louis, MO, USA) and NOF (Tokyo, Japan), respectively. RPMI-1640 was purchased from Nissui Pharmaceutical (Tokyo, Japan) and fetal bovine serum (FBS) was purchased from Japan Bioserum (Hiroshima, Japan). All other chemicals were of the highest purity available.

2.2. pDNA, cell lines and mice

pCMV-Luc was constructed as described previously [33]. Briefly, the HindIII/Xba I firefly luciferase cDNA fragment from pGL3-control vector (Promega, Madison, WI, USA) was sub-cloned into the polylinker of pcDNA3 vector (Invitrogen, Carlsbad, CA, USA). Pathway profiling luciferase systems (pTA/Luc, pAP-1/Luc, pNFκB/Luc, pCRE/Luc and pSRE/Luc) were purchased from Clontech Laboratories (Mountain View, CA, USA). pDNA was amplified in the *Escherichia coli* strain DH5α, isolated and purified using a QIAGEN Endofree Plasmid Giga Kit (QIAGEN, Hilden, Germany). RAW264.7 cells, from a murine macrophage-like cell line, were cultured in RPMI-1640 supplemented with 10% FBS, 100 IU/ml penicillin, 100 μg/ml streptomycin, and 2 mM L-glutamine. Cells were plated onto 24-well culture plates at a density of 5×10^4 cells/1.88 cm^2 at 37 °C in 5% CO_2, and incubated for 48 h prior to experiments. Female ICR mice (4-week-old) and female C57BL/6 mice (6-week-old) were purchased from Japan SLC (Shizuoka, Japan). All animal experiments were carried out in accordance with the Principles of Laboratory Animal Care, as adopted and propagated by the U.S. National Institutes of Health and the Kyoto University Guidelines for Animal Experiments.

2.3. Construction of Man-PEG_{2000} bubble lipoplexes

Man-PEG_{2000} bubble lipoplexes were constructed according to our previous report [17]. Briefly, DSTAP, DSPC, and NH_2-PEG_{2000}-DSPE or mannose-modified PEG_{2000}-DSPE were mixed in chloroform at a molar ratio of 7:2:1 to produce the liposomes for bubble lipoplexes. The liposome construction mixture was dried by evaporation and vacuum desiccated before the resultant lipid film was resuspended in sterile 5% dextrose. After hydration for 30 min at 65 °C, the dispersion was sonicated for 10 min in a bath sonicator and 3 min in a tip sonicator for liposome production. Liposomes were then sterilized by passage through a 0.45 μm filter (PALL, East Hills, NY, USA). Lipoplexes were prepared by gently mixing with equal volumes of pDNA and liposome solution at a charge ratio of 1.0:2.3 (−:+). Prepared lipoplexes were pressurized with perfluoropropane gas (Takachiho Chemical Industries, Tokyo, Japan) and sonicated using a bath-type sonicator (AS ONE, Osaka, Japan) for 5 min to enclose US imaging gas. Particle sizes and ζ-potentials of the liposomes/lipoplexes were determined using a Zetasizer Nano ZS instrument (Malvern Instrument, Worcestershire, UK).

2.4. Harvesting of mouse peritoneal macrophages

Mouse peritoneal macrophages were harvested and cultured as previously described [34]. Briefly, the macrophages were harvested from the peritoneal cavity of female ICR mice, before being washed and suspended in RPMI-1640 medium supplemented with 10% FBS, 100 IU/ml penicillin, 100 μg/ml streptomycin and 2 mM L-glutamine, and plated onto 24-well culture plates at a density of 2×10^5 cells/1.88 cm^2. After incubation for 2 h at 37 °C in 5% CO_2, non-adherent cells were washed off with culture medium, and the macrophages were incubated for another 72 h.

2.5. In vitro gene transfection

After RAW264.7 cells and macrophages were plated and incubated for 48 and 72 h, respectively, the culture medium was replaced with Opti-MEM I containing bubble lipoplexes (5 μg pDNA). Cells were exposed to US (frequency, 2.062 MHz; duty, 50%; burst rate, 10 Hz; intensity 4.0 W/cm^2) for 20 s using a Sonopore-4000 sonicator (NEPA GENE, Chiba, Japan) with a 6 mm diameter probe placed in each well at predetermined times after the addition of bubble lipoplexes. At 1 h after addition of bubble lipoplexes, the incubation medium was replaced with RPMI-1640 and incubated for an additional time. Subsequently, the cells were scraped from the plates and suspended in lysis buffer (0.05% Triton X-100, 2 mM EDTA, 0.1 M Tris, pH 7.8). The cell suspension was shaken, and centrifuged at 10,000×g, 4 °C for 10 min. Luciferase assay buffer (Picagene; Toyo Ink, Tokyo, Japan) was mixed with the supernatant and the luciferase activity was measured in a luminometer (Lumat LB 9507; EG&G Berthold, Bad Wildbad, Germany). Luciferase activity was normalized against the cellular protein content. Protein concentration was determined with a Protein Quantification Kit (Dojindo Molecular Technologies, Tokyo, Japan).

2.6. In vivo gene transfection

Mice were intravenously injected with 400 μl of bubble lipoplexes via the tail vein using a 26-gauge syringe needle at a dose of 50 μg pDNA. At predetermined times after the injection, US (frequency, 1.045 MHz; duty, 50%; burst rate, 10 Hz; intensity 1.0 W/cm^2; time, 2 min) was exposed transdermally to the abdominal area using a Sonopore-4000 sonicator (NEPA GENE) with a 20 mm diameter probe. At predetermined times after injection, mice were sacrificed and organs were collected for each experiment. Organs were washed twice with cold saline and homogenized with lysis buffer (0.05% Triton X-100, 2 mM EDTA, 0.1 M Tris, pH 7.8). Lysis buffer was added at a weight ratio of 5 ml/g for the liver or 4 ml/g for other organs. After 3 cycles of freezing and thawing, the homogenates were centrifuged at 10,000×g at 4 °C for 10 min. Luciferase activity of the resulting supernatant was determined by above-mentioned luciferase assay.

2.7. Quantitative reverse transcription-polymerase chain reaction (RT-PCR)

Total ribonucleic acid (RNA) was isolated from the cells and organs using a GenElute Mammalian Total RNA Miniprep Kit (Sigma-Aldrich). Reverse transcription of messenger RNA (mRNA) was carried out using PrimeScript® RT reagent Kit (Takara Bio, Shiga, Japan). The detection of complementary deoxyribonucleic acid (cDNA) (*c-fos*, *c-jun*, *p105*, *p65* and *gapdh*) was conducted using real-time PCR using SYBR® Premix Ex Taq (Takara Bio) and a Lightcycler Quick System 350S (Roche Diagnostics, Indianapolis, IN, USA). Primers for *c-fos*, *c-jun*, *p105*, *p65* and *gapdh* cDNA were synthesized by Sigma-Aldrich as follows: *c-fos*, 5′-CCA GTC AAG AGC ATC AGC AA-3′ (forward) and 5′-AAG TAG TGC AGC CCG GAG TA-3′ (reverse); *c-jun*, 5′-TCC CCT ATC GAC ATG GAG TC-3′ (forward) and 5′-TGA GTT GGC ACC CAC TGT TA-3′ (reverse); *p105*, 5′-CCT GGA TGA CTC TTG GGA AA-3′ (forward) and 5′-TCA GCC AGC TGT TTC ATG TC-3′ (reverse); *p65*, 5′-TAG CAC CTG ATG GCT GAC TG-3′ (forward) and 5′-CGT TCC ACC ACA TCT GTG TC-3′ (reverse); *gapdh*, 5′-TCT CCT GCG ACT TCA ACA-3′ (forward) and 5′-GCT GTA GCC GTA TTC ATT GT-3′ (reverse). mRNA copy number was calculated for each sample from the standard curve using the thermal-cycler software ('Arithmetic Fit Point analysis' for the Lightcycler). Results were expressed as relative copy number calculated relative to *gapdh* mRNA (*c-fos*, *c-jun*, *p105*, *p65* mRNA copy number/*gapdh* mRNA copy number).

2.8. Measurement of the level of intranuclear protein

Cells and tissues were collected at predetermined times after gene transfection, and the nuclear extract from cells and tissues was prepared using a Nuclear Extract Kit (Active Motif, Carlsbad, CA, USA). Nuclear protein was divided into aliquots and stored at −80 °C for later use. The protein concentration was measured with a Protein Quantification Kit. The amounts of p50 and p65, which are the components of NFκB in the cellular nuclear extract was measured using a NFκB (p50) Transcription Factor Kit (Thermo Fisher Scientific, Waltham, MA, USA) and a NFκB (p65) transcription Factor Assay Kit (Cayman Chemical, Ann Arbor, MI, USA), respectively, according to the manufacturer's protocols.

2.9. Measurement of inflammatory cytokines

At predetermined times after the in vitro and in vivo gene transfection, the supernatants and serum were collected and the cytokine levels (TNF-α, IFN-γ, and IL-6) were determined with a commercial enzyme-linked immunosorbent assay (ELISA) Kit (Bay Bioscience, Hyogo, Japan) according to the recommended procedures.

2.10. Statistical analysis

Results were presented as the mean ± S.D. of more than three experiments. Analysis of variance (ANOVA) was used to test the statistical significance of differences among groups. Two-group comparisons were performed by Student's *t*-test. Multiple comparisons between control and test groups were performed by Dunnett's test and multiple comparisons between all groups were performed using the Tukey–Kramer test.

3. Results

3.1. Physicochemical properties of lipoplexes and bubble lipoplexes used in this study

The physicochemical properties of lipoplexes and bubble lipoplexes constructed with various pDNAs used in all experiments were evaluated by measuring the particle sizes and ζ-potentials. Mean particle sizes and ζ-potentials of unmodified and Man-PEG_{2000} lipoplexes were approximately 137 nm and +48 mV, respectively (Supplementary Table 1). Moreover, mean particle sizes and ζ-potentials of unmodified and Man-PEG_{2000} bubble lipoplexes were approximately 550 nm and +48 mV, respectively (Supplementary Table 1). These results correspond to previous reports [17–19]; suggesting that these pDNA had no effect on the physicochemical properties of lipoplexes and bubble lipoplexes.

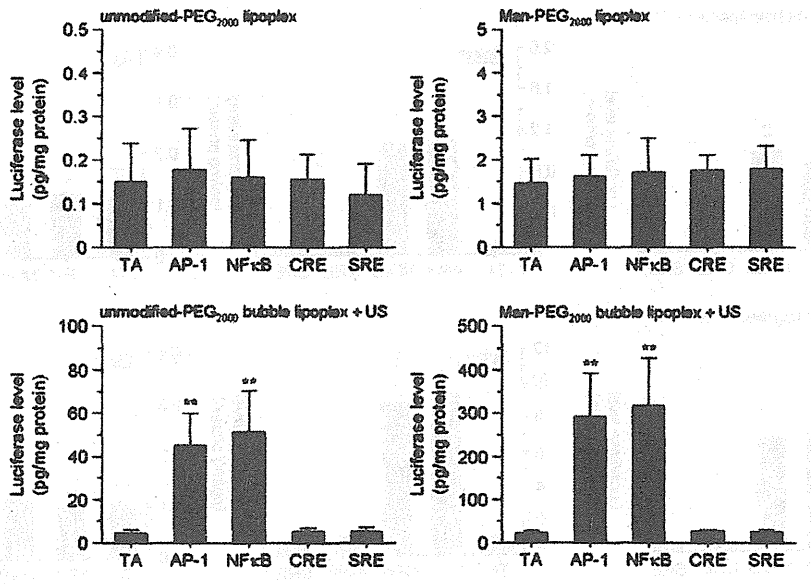

Fig. 1. The effect of transcriptional factors on gene expression obtained by unmodified and Man-PEG_{2000} bubble lipoplexes with or without US exposure in mouse cultured macrophages. Luciferase expression levels obtained by unmodified-PEG_{2000} lipoplexes, Man-PEG_{2000} lipoplexes, unmodified-PEG_{2000} bubble lipoplexes with US exposure, and Man-PEG_{2000} bubble lipoplexes with US exposure (5 μg of pDNA) at 24 h after transfection in mouse primary cultured macrophages. Lipoplexes were constructed with pDNAs controlled by various transcription factors. Each value represents the mean + S.D. ($n = 4$). Key: TA; pTA/Luc, AP-1; pAP-1/Luc, NFκB; pNFκB/Luc, CRE; pCRE/Luc, SRE; pSRE/Luc. $^{**}p < 0.01$, compared with the corresponding TA group.

3.2. Involvement of transcriptional process on enhanced gene expression obtained by unmodified and Man-PEG$_{2000}$ bubble lipoplexes with US exposure in vitro

The involvement of transcription on enhanced gene expression obtained by unmodified and Man-PEG$_{2000}$ bubble lipoplexes with US exposure was investigated in mouse primary cultured macrophages. First, we examined gene expression levels using unmodified/Man-PEG$_{2000}$ lipoplexes or bubble lipoplexes constructed with luciferase expressing-pDNA controlled by various transcription factors, including AP-1, NFκB, CRE and SRE. Gene expression levels obtained by Man-PEG$_{2000}$ lipoplexes only or Man-PEG$_{2000}$ bubble lipoplexes with US exposure were higher than those by unmodified-PEG$_{2000}$ formulations (Fig. 1), since mouse cultured macrophages express the mannose receptors abundantly. Moreover, although the level of gene expression obtained by both lipoplexes was similar in all pDNAs, the level of gene expression obtained by both bubble lipoplexes and US exposure was enhanced approximately 10-fold by gene transfection using pAP-1/Luc and pNFκB/Luc, compared with that using pTA/Luc, which is a pDNA without transcription factor-binding site within the enhancer region (Fig. 1). Similar results were observed in the murine macrophage-like RAW264.7 cells (Supplementary Fig. 1).

3.3. Involvement of transcriptional process on enhanced gene expression obtained by unmodified and Man-PEG$_{2000}$ bubble lipoplexes with US exposure in mice

Next, we investigated the level of gene expression by in vivo gene transfection using unmodified/Man-PEG$_{2000}$ lipoplexes and bubble lipoplexes constructed with luciferase expressing-pDNA controlled by

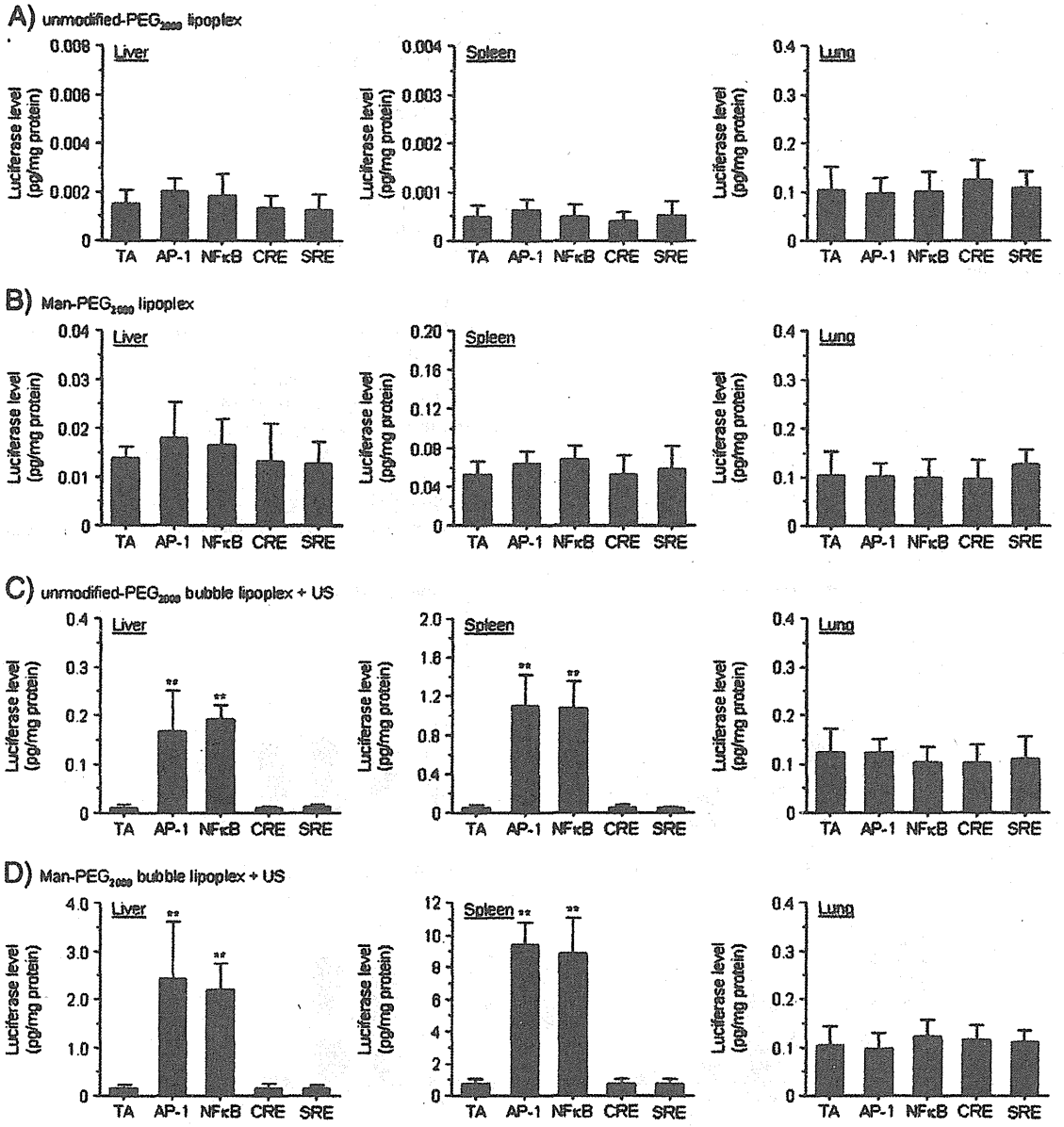

Fig. 2. The effect of transcriptional factors on gene expression obtained by unmodified and Man-PEG$_{2000}$ bubble lipoplexes with or without US exposure in vivo. Luciferase expression levels obtained by unmodified-PEG$_{2000}$ lipoplexes (A), Man-PEG$_{2000}$ lipoplexes (B), unmodified-PEG$_{2000}$ bubble lipoplexes with US exposure (C), and Man-PEG$_{2000}$ bubble lipoplexes with US exposure (D) (50 μg of pDNA) in the liver, spleen and lung at 6 h after transfection. Lipoplexes were constructed with pDNAs controlled by various types of transcriptional factors. Each value represents the mean + S.D. ($n=4$). Key: TA; pTA/Luc, AP-1; pAP-1/Luc, NFκB; pNFκB/Luc, CRE; pCRE/Luc, SRE; pSRE/Luc. $^{**}p<0.01$, compared with the corresponding TA group.

various transcription factors. Gene expression levels in the liver and spleen obtained by Man-PEG_{2000} lipoplexes only or Man-PEG_{2000} bubble lipoplexes with US exposure were higher than those by unmodified-PEG_{2000} formulations (Fig. 2), since liver and spleen are the major target organ of mannose-modified carriers. Although the level of gene expression obtained by both lipoplexes was similar in all pDNAs (Fig. 2A and B), gene expression levels in the liver and spleen obtained by both bubble lipoplexes and US exposure were enhanced approximately 10-fold by gene transfection using pAP-1/Luc and pNFκB/Luc, compared with that using pTA/Luc (Fig. 2C and D). On the other hand, enhanced gene expression followed by gene transfection using bubble lipoplexes constructed with pAP-1/Luc or pNFκB/Luc was not observed in the lung.

3.4. The effect of in vitro gene transfection using unmodified and Man-PEG_{2000} bubble lipoplexes with US exposure on AP-1 and NFκB

Following examination of the expression properties for c-fos and c-jun, which are the components of AP-1, *c-fos* and *c-jun* mRNA expression was enhanced transiently in mouse primary cultured macrophages by not only the gene transfection using bubble lipoplexes and US exposure, but also US exposure alone (Fig. 3A). Moreover, enhanced expression of *c-fos* and *c-jun* mRNA was not observed in the gene transfection using lipoplexes only (Fig. 3A). Evaluation of the expressing properties and intranuclear transporting properties of NFκB followed by gene transfection revealed that *p105* (precursor of p50) and *p65* mRNA expression in mouse primary cultured macrophages was not enhanced in all of groups, which differed from the results obtained for *c-fos* and *c-jun* mRNA (Supplementary Fig. 2). In contrast, the amount of intranuclear p50 and p65 increased transiently by not only the gene transfection using bubble lipoplexes and US exposure, but also US exposure alone (Fig. 3B). On the other hand, enhanced intranuclear transport of p50 and p65 was not observed in the gene transfection using lipoplexes only (Fig. 3B). Moreover, these transient AP-1 expression and intranuclear transport of NFκB followed by US exposure were also observed in RAW264.7 cells in this gene transfection method (Supplementary Fig. 3). These results suggest that transcription activation, such as increased AP-1 expression and enhanced intranuclear transport of NFκB, is partly involved in enhanced gene expression produced by unmodified and Man-PEG_{2000} bubble lipoplexes with US exposure.

3.5. The effect of in vivo gene transfection using unmodified and Man-PEG_{2000} bubble lipoplexes with US exposure on AP-1 and NFκB

c-fos/c-jun mRNA expression and the intranuclear amount of p50/p65 were enhanced transiently by not only the gene transfection using bubble lipoplexes and US exposure, but also US exposure alone in both the liver and spleen (Figs. 4 and 5). On the other hand, these phenomena were not observed in the lung (Figs. 4C and 5C). In addition, *c-fos* and *c-jun* mRNA expression levels in the liver and spleen followed by US exposure were dependedent on the US intensity (Supplementary Fig. 4).

3.6. The effect of in vitro and in vivo gene transfection using unmodified and Man-PEG_{2000} bubble lipoplexes and US exposure on inflammatory cytokine production

Increased AP-1 expression and intranuclear transport of NFκB followed by US exposure were demonstrated to be involved in the enhanced gene expression by unmodified and Man-PEG_{2000} bubble lipoplexes with US exposure. On the other hand, since these phenomena are potentially involved in the production of inflammatory cytokines [31,32], the production properties of inflammatory cytokines followed by gene transfection were investigated in vitro and in vivo. Although TNF-αproduction followed by gene transfection using only lipoplexes was significantly increased time-dependently in RAW264.7 cells and mouse primary cultured macrophages, only a slight increase in TNF-α production was observed followed by gene transfection using bubble lipoplexes and US exposure (Fig. 6).

While the inflammatory cytokines (TNF-α, IFN-γ, and IL-6) in the serum followed by in vivo gene transfection exhibited transient and significant increases in all of gene transfection methods (Fig. 7), the

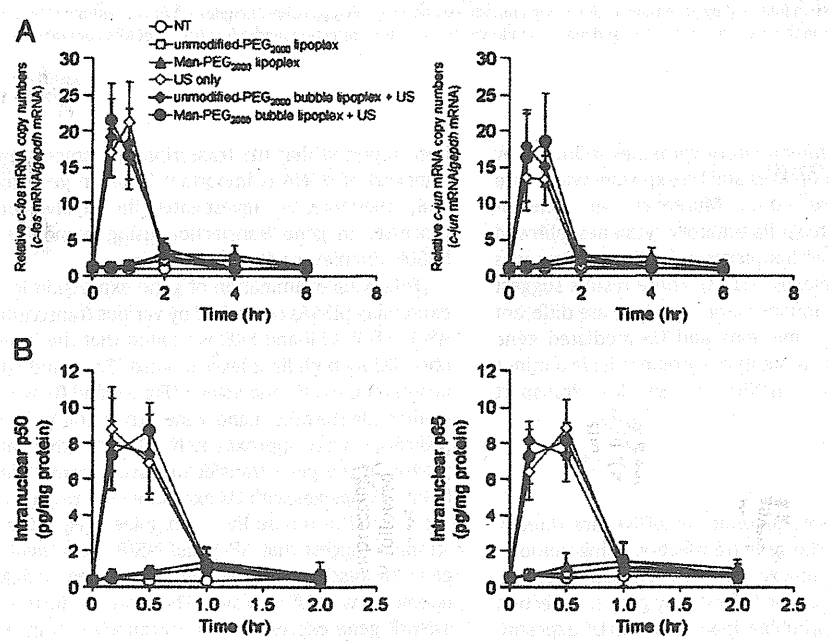

Fig. 3. Enhanced *c-fos/c-jun* mRNA expression and intranuclear transport of p105/p65 followed by gene transfection using unmodified and Man-PEG_{2000} bubble lipoplexes with or without US exposure in mouse primary cultured macrophages. Time-course of *c-fos/c-jun* mRNA expression levels (A) and intranuclear p105/p65 levels (B) followed by various transfection methods (5 μg of pCMV-Luc) in mouse primary cultured macrophages. Each value represents the mean ± S.D. ($n = 4$). $^{**}p<0.01$, compared with the corresponding non-treatment (NT) group.

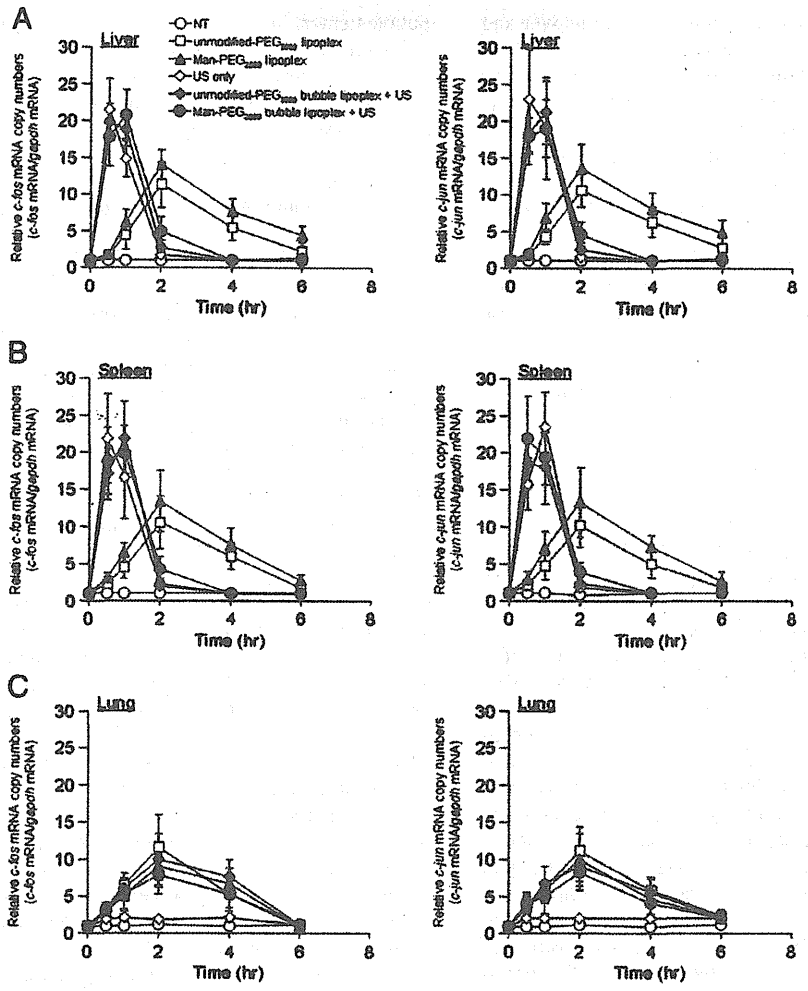

Fig. 4. Enhanced *c-fos/c-jun* mRNA expression followed by gene transfection using unmodified and Man-PEG_{2000} bubble lipoplexes with or without US exposure in vivo. Time-course of *c-fos* and *c-jun* mRNA expression levels in the liver (A), spleen (B), and lung (C) followed by various transfection methods (50 μg of pCMV-Luc) in mice. Each value represents the mean ± S.D. ($n = 4$). NT: non-treatment.

maximum amount of secreted inflammatory cytokines followed by gene transfection using bubble lipoplexes and US exposure was 3-fold lower than that using lipoplexes only. Moreover, the time-to-maximum concentration of secreted inflammatory cytokines followed by gene transfection using bubble lipoplexes and US exposure was earlier than that using only lipoplexes (Fig. 7). These results suggest that the production properties of inflammatory cytokine are different between conventional lipofection methods and US-mediated gene transfection methods, and that inflammatory cytokines have a minor effect on enhanced AP-1 expression/NFκB intranuclear transport followed by US exposure.

4. Discussion

We recently reported that large amounts of pDNA are directly transferred into the cytoplasm in the gene transfection using unmodified and Man-PEG_{2000} bubble lipoplexes with US exposure [17,19]. However, this enhanced gene expression followed by gene transfection using unmodified and Man-PEG_{2000} bubble lipoplexes with US exposure may not correspond to the increase of intracellular pDNA by targeted delivery of pDNA and intracytoplasmic transfer of pDNA; suggesting the involvement of the other factors on the enhanced gene expression in the gene transfection using both bubble lipoplexes and US exposure. It has been reported that the transcriptional process following intranuclear transport of pDNA is important factor in gene transfection efficiency [7,8]; therefore, we investigated the involvement of transcriptional processes in gene transfection using unmodified and Man-PEG_{2000} bubble lipoplexes with US exposure.

Following examination of gene expression levels using luciferase-expressing pDNAs controlled by various transcription factors, including AP-1, NFκB, CRE and SRE, we found that the level of gene expression obtained by both lipoplexes in vitro (Fig. 1 and Supplementary Fig. 1), and in mouse liver and spleen (Fig. 2A and B), was similar in all pDNAs studied. On the other hand, gene expression levels using pAP-1/Luc and pNFκB/Luc were approximately 10-fold higher than those using other pDNAs in the gene transfection using unmodified and Man-PEG_{2000} bubble lipoplexes with US exposure in vitro (Fig. 1 and Supplementary Fig. 1), and in mouse liver and spleen (Fig. 2C and D). These results strongly suggest that AP-1 and NFκB were involved in the enhanced gene expression obtained by unmodified and Man-PEG_{2000} bubble lipoplexes with US exposure. Therefore, we further investigated the AP-1/NFκB gene expression and intranuclear transport followed by this gene transfection method.

c-fos/c-jun mRNA expression (Figs. 3A and 4) and intranuclear p50/p65 levels (Figs. 3B and 5) were enhanced transiently by not only the gene transfection using both bubble lipoplexes and US exposure,

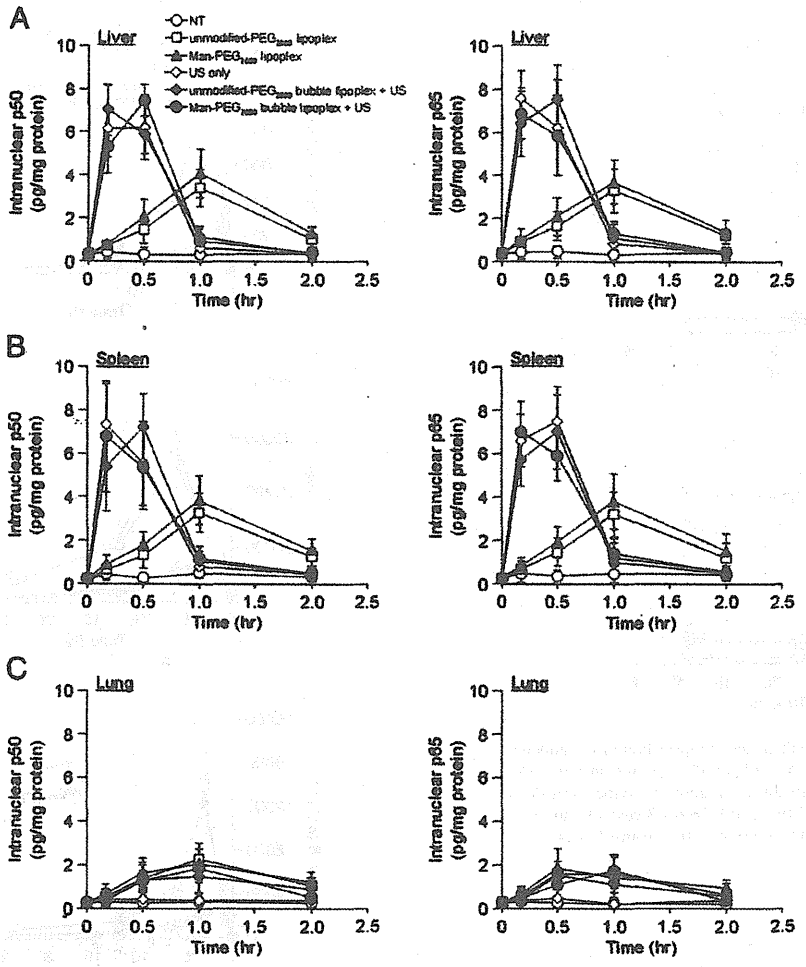

Fig. 5. Enhanced intranuclear transport of p50 and p65 followed by gene transfection using unmodified and Man-PEG_{2000} bubble lipoplexes with or without US exposure in vivo. Time-course of intranuclear p50 and p65 levels in the liver (A), spleen (B), and lung (C) followed by various transfection methods (50 μg of pCMV-Luc) in mice. Each value represents the mean ± S.D. ($n = 3$). NT; non-treatment.

but also US exposure alone in vitro, and in mouse liver and spleen. It has been reported that US exposure induced the enhanced expression of c-fos and c-jun via phosphorylation of ERK, p38 and JNK [25,26], and our results partially correspond to these reports. These observations led us to believe that the activation of AP-1 and NFκB-mediated transcriptional processes followed by US exposure is involved in the enhanced gene expression using unmodified and Man-PEG_{2000} bubble lipoplexes with US exposure.

Since the activation of transcription factors such as AP-1 [28] and NFκB [29,30] is involved in the induction of inflammatory responses [31,32], we investigated the production properties of inflammatory cytokines followed by this gene transfection method. The production levels of TNF-α, IFN-γ or IL-6 followed by gene transfection using both bubble lipoplexes and US exposure were substantially lower than that using both lipoplexes in vitro (Fig. 6) and in vivo (Fig. 7). We previously reported that the inflammatory responses were significantly suppressed in the gene transfection method using unmodified and Man-PEG_{2000} bubble lipoplexes with US exposure, because a large amount of pDNA was transferred into the cytoplasm directly through the transient pores created by the destruction of both bubble lipoplexes followed by US exposure [19], suggesting that pDNA is hardly interacted with endosomal TLR-9. On the other hand, it was reported that the phosphorylation of AP-1 and NFκB was induced via the activation of p38, ERK and JNK-mediated pathways followed by US exposure [25,26], and we showed that these AP-1 and NFκB activation was transiently in our sonoporation method and condition in this study (Figs. 3–5 and Supplementary Fig. 3). Although these activation of AP-1 and NFκB leads to the inflammatory cytokine production [31,32], the inflammatory responses induced by AP-1 and NFκB activation followed by US exposure were low under in vitro and in vivo condition (Figs. 6 and 7). We previously have reported that the activating level of transcriptional factors, such as c-fos and c-jun, in tissue pressure-mediated transfection method was approximately one-fifth, compared with that in hydrodynamics method [22]. Moreover, the production of inflammatory cytokines under in vivo condition followed by tissue pressure-mediated transfection method was much lower than those by conventional lipofection method [35]. The activating levels of transcriptional factors followed by our sonoporation method using unmodified and Man-PEG_{2000} bubble lipoplexes with US exposure were almost the same with that by tissue pressure-mediated transfection method. Therefore, the contribution of the inflammatory response induced by AP-1 and NFκB activation followed by our sonoporation method may be negligible. These results suggest that the transient expression of AP-1 and the transient intranuclear transport of NFκB followed by US exposure might be minimally involved in the inflammatory responses in the gene transfection using unmodified and Man-PEG_{2000} bubble lipoplexes with US exposure.

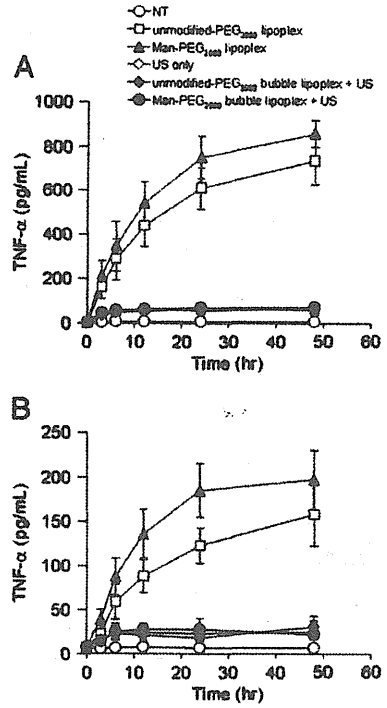

Fig. 6. Evaluation of TNF-α secretion followed by gene transfection using unmodified and Man-PEG_{2000} bubble lipoplexes with or without US exposure in vitro. TNF-α concentration in the supernatant was measured following various transfection methods (5 μg of pDNA) at predetermined times in RAW264.7 cells (A) and mouse primary cultured macrophages (B). Each value represents the mean ± S.D. ($n = 4$).

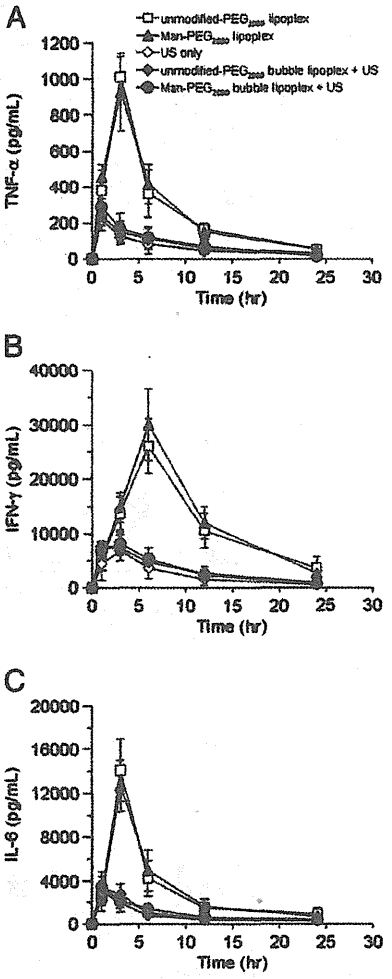

Fig. 7. Evaluation of pro-inflammatory cytokine secretion in serum followed by gene transfection using unmodified and Man-PEG_{2000} bubble lipoplexes with or without US exposure in vivo. TNF-α (A), IFN-γ (B), and IL-6 (C) concentrations in the serum were measured following various transfection methods (50 μg of pDNA) at predetermined times in mice. Each value represents the mean ± S.D. ($n = 4$).

5. Conclusion

Our results suggest that the activated AP-1 and NFκB followed by US exposure is involved in the enhanced gene expression using unmodified and Man-PEG_{2000} bubble lipoplexes with US exposure. These results suggest that enhanced gene expression in the gene transfection using our sonoporation method was obtained by applying pDNA controlled by the specific transcriptional factors. Therefore, the selection of suitable pDNA with specific promoter regions activated by US stimulation is one of the important factors for efficient gene expression in our gene transfection method. In addition, the transient expression of AP-1 and the transient intranuclear transport of NFκB followed by US exposure were not substantially involved in the inflammatory responses in this gene transfection method. These findings may help in the development of an effective gene transfection method using US-exposing system.

Acknowledgments

This work was supported in part by a Grant-in-Aid for Young Scientists (A) from the Ministry of Education, Culture, Sports, Science and Technology of Japan, and by Health and Labour Sciences Research Grants for Research on Noninvasive and Minimally Invasive Medical Devices from the Ministry of Health, Labour and Welfare of Japan, and by the Programs for Promotion of Fundamental Studies in Health Sciences of the National Institute of Biomedical Innovation (NIBIO).

Appendix A. Supplementary data

Supplementary data to this article can be found online at doi:10.1016/j.jconrel.2011.06.040.

References

[1] M. Thomas, A.M. Klibanov, Non-viral gene therapy: polycation-mediated DNA delivery, Appl. Microbiol. Biotechnol. 2003 (2003) 27–34.
[2] T. Ito, N. Iida-Tanaka, T. Niidome, T. Kawano, K. Kubo, K. Yoshikawa, T. Sato, Z. Yang, Y. Koyama, Hyaluronic acid and its derivative as a multi-functional gene expression enhancer: protection from non-specific interactions, adhesion to targeted cells, and transcriptional activation, J. Control. Release 112 (2006) 382–388.
[3] D.G. Miller, P.R. Wang, L.M. Petek, R.K. Hirata, M.S. Sands, D.W. Russell, Gene targeting in vivo by adeno-associated virus vectors, Nat. Biotechnol. 24 (2006) 1022–1026.
[4] K. Itaka, K. Yamauchi, A. Harada, K. Nakamura, H. Kawaguchi, K. Kataoka, Polyion complex micelles from plasmid DNA and poly(ethylene glycol)-poly(L-lysine) block copolymer as serum-tolerable polyplex system: physicochemical properties of micelles relevant to gene transfection efficiency, Biomaterials 24 (2003) 4495–4506.
[5] A. Kim, E.H. Lee, S.H. Choi, C.K. Kim, In vitro and in vivo transfection efficiency of a novel ultradeformable cationic liposome, Biomaterials 25 (2004) 305–313.
[6] S.M. Kwon, H.Y. Nam, T. Nam, K. Park, S. Lee, K. Kim, I.C. Kwon, J. Kim, D. Kang, J.H. Park, S.Y. Jeong, In vivo time-dependent gene expression of cationic lipid-based emulsion as a stable and biocompatible non-viral gene carrier, J. Control. Release 128 (2008) 89–97.
[7] S. Hama, H. Akita, R. Ito, H. Mizuguchi, T. Hayakawa, H. Harashima, Quantitative comparison of intracellular trafficking and nuclear transcription between adenoviral and lipoplex systems, Mol. Ther. 13 (2006) 786–794.
[8] S. Hama, H. Akita, S. Iida, H. Mizuguchi, H. Harashima, Quantitative and mechanism-based investigation of post-nuclear delivery events between adenovirus and lipoplex, Nucleic Acids Res. 35 (2007) 1533–1543.

[9] H. Potter, L. Weir, P. Leder, Enhancer-dependent expression of human kappa immunoglobulin genes introduced into mouse pre-B lymphocytes by electroporation, Proc. Natl. Acad. Sci. U.S.A. 81 (1984) 7161–7165.
[10] F. Liu, Y. Song, D. Liu, Hydrodynamics-based transfection in animals by systemic administration of plasmid DNA, Gene Ther. 6 (1999) 1258–1266.
[11] Y. He, A.A. Pimenov, J.V. Nayak, J. Plowey, L.D. Falo Jr., L. Huang, Intravenous injection of naked DNA encoding secreted flt3 ligand dramatically increases the number of dendritic cells and natural killer cells in vivo, Hum. Gene Ther. 11 (2000) 547–554.
[12] F. Liu, L. Huang, Noninvasive gene delivery to the liver by mechanical massage, Hepatology 35 (2002) 1314–1319.
[13] K. Anwer, G. Kao, B. Proctor, I. Anscombe, V. Florack, R. Earls, E. Wilson, T. McCreery, E. Unger, A. Rolland, S.M. Sullivan, Ultrasound enhancement of cationic lipid-mediated gene transfer to primary tumors following systemic administration, Gene Ther. 7 (2000) 1833–1839.
[14] G. Zhang, X. Gao, Y.K. Song, R. Vollmer, D.B. Stolz, J.Z. Gasiorowski, D.A. Dean, D. Liu, Hydroporation as the mechanism of hydrodynamic delivery, Gene Ther. 11 (2004) 675–682.
[15] Y. Negishi, Y. Endo, T. Fukuyama, R. Suzuki, T. Takizawa, D. Omata, K. Maruyama, Y. Aramaki, Delivery of siRNA into the cytoplasm by liposomal bubbles and ultrasound, J. Control. Release 132 (2008) 124–130.
[16] I. Lentacker, N. Wang, R.E. Vandenbroucke, J. Demeester, S.C. De Smedt, N.N. Sanders, Ultrasound exposure of lipoplex loaded microbubbles facilitates direct cytoplasmic entry of the lipoplexes, Mol. Pharm. 6 (2009) 457–467.
[17] K. Un, S. Kawakami, R. Suzuki, K. Maruyama, F. Yamashita, M. Hashida, Development of an ultrasound-responsive and mannose-modified gene carrier for DNA vaccine therapy, Biomaterials 31 (2010) 7813–7826.
[18] K. Un, S. Kawakami, R. Suzuki, K. Maruyama, F. Yamashita, M. Hashida, Suppression of melanoma growth and metastasis by DNA vaccination using an ultrasound-responsive and mannose-modified gene carrier, Mol. Pharm. 8 (2011) 543–554.
[19] K. Un, S. Kawakami, M. Yoshida, Y. Higuchi, R. Suzuki, K. Maruyama, F. Yamashita, M. Hashida, The elucidation of gene transferring mechanism by ultrasound-responsive unmodified and mannose-modified lipoplexes, Biomaterials 32 (2011) 4659–4669.
[20] T. Pazmany, S.P. Murphy, S.O. Gollnick, S.P. Brooks, T.B. Tomasi, Activation of multiple transcription factors and fos and jun gene family expression in cells exposed to a single electric pulse, Exp. Cell Res. 221 (1995) 103–110.
[21] M. Nishikawa, A. Nakayama, Y. Takahashi, Y. Fukuhara, Y. Takakura, Reactivation of silenced transgene expression in mouse liver by rapid, large-volume injection of isotonic solution, Hum. Gene Ther. 19 (2008) 1009–1020.
[22] H. Mukai, S. Kawakami, H. Takahashi, K. Satake, F. Yamashita, M. Hashida, Key physiological phenomena governing transgene expression based on tissue pressure-mediated transfection in mice, Biol. Pharm. Bull. 33 (2010) 1627–1632.
[23] T. Tanos, M.J. Marinissen, F.C. Leskow, D. Hochbaum, H. Martinetto, J.S. Gutkind, O.A. Coso, Phosphorylation of c-Fos by members of the p38 MAPK family. Role in the AP-1 response to UV light, J. Biol. Chem. 280 (2005) 18842–18852.
[24] S. Ramanan, M. Kooshki, W. Zhao, F.C. Hsu, M.E. Robbins, PPARalpha ligands inhibit radiation-induced microglial inflammatory responses by negatively regulating NF-kappaB and AP-1 pathways, Free Radic. Biol. Med. 45 (2008) 1695–1704.
[25] Y.C. Chiu, T.H. Huang, W.M. Fu, R.S. Yang, C.H. Tang, Ultrasound stimulates MMP-13 expression through p38 and JNK pathway in osteoblasts, J. Cell. Physiol. 215 (2008) 356–365.
[26] S. Zhou, M.G. Bachem, T. Seufferlein, Y. Li, H.J. Gross, A. Schmelz, Low intensity pulsed ultrasound accelerates macrophage phagocytosis by a pathway that requires actin polymerization, Rho, and Src/MAPKs activity, Cell. Signal. 20 (2008) 695–704.
[27] H. Ochiai, M. Fujimuro, H. Yokosawa, H. Harashima, H. Kamiya, Transient activation of transgene expression by hydrodynamics-based injection may cause rapid decrease in plasmid DNA expression, Gene Ther. 14 (2007) 1152–1159.
[28] R. Eferl, E.F. Wagner, AP-1: a double-edged sword in tumorigenesis, Nat. Rev. Cancer 3 (2003) 859–868.
[29] N.D. Perkins, Integrating cell-signalling pathways with NF-kappaB and IKK function, Nat. Rev. Mol. Cell Biol. 8 (2007) 49–62.
[30] S.G. Pereira, F. Oakley, Nuclear factor-kappaB1: regulation and function, Int. J. Biochem. Cell Biol. 40 (2008) 1425–1430.
[31] A. Cloutier, T. Ear, O. Borissevitch, P. Larivée, P.P. McDonald, Inflammatory cytokine expression is independent of the c-Jun N-terminal kinase/AP-1 signaling cascade in human neutrophils, J. Immunol. 171 (2003) 3751–3761.
[32] A.M. Elsharkawy, D.A. Mann, Nuclear factor-kappaB and the hepatic inflammation-fibrosis-cancer axis, Hepatology 46 (2007) 590–597.
[33] T. Takagi, M. Hashiguchi, R.I. Mahato, H. Tokuda, Y. Takakura, M. Hashida, Involvement of specific mechanism in plasmid DNA uptake by mouse peritoneal macrophages, Biochem. Biophys. Res. Commun. 245 (1998) 729–733.
[34] K. Un, S. Kawakami, R. Suzuki, K. Maruyama, F. Yamashita, M. Hashida, Enhanced transfection efficiency into macrophages and dendritic cells by a combination method using mannosylated lipoplexes and bubble liposomes with ultrasound exposure, Hum. Gene Ther. 21 (2010) 65–74.
[35] H. Mukai, S. Kawakami, Y. Kamiya, F. Ma, H. Takahashi, K. Satake, K. Terao, H. Kotera, F. Yamashita, M. Hashida, Pressure-mediated transfection of murine spleen and liver, Hum. Gene Ther. 20 (2009) 1157–1167.

molecular pharmaceutics

ARTICLE

pubs.acs.org/molecularpharmaceutics

Suppression of Melanoma Growth and Metastasis by DNA Vaccination Using an Ultrasound-Responsive and Mannose-Modified Gene Carrier

Keita Un,[†,‡] Shigeru Kawakami,[*,†] Ryo Suzuki,[§] Kazuo Maruyama,[§] Fumiyoshi Yamashita,[†] and Mitsuru Hashida[*,†,∥]

[†]Department of Drug Delivery Research, Graduate School of Pharmaceutical Sciences, Kyoto University, 46-29 Yoshida-shimoadachi-cho, Sakyo-ku, Kyoto 606-8501, Japan

[‡]The Japan Society for the Promotion of Science (JSPS), Chiyoda-ku, Tokyo 102-8471, Japan

[§]Department of Biopharmaceutics, School of Pharmaceutical Sciences, Teikyo University, 1091-1 Suwarashi, Midori-ku, Sagamihara, Kanagawa 252-5195, Japan

[∥]Institute for Integrated Cell-Material Sciences (iCeMS), Kyoto University, Yoshida-ushinomiya-cho, Sakyo-ku, Kyoto 606-8302, Japan

Supporting Information

ABSTRACT: DNA vaccination has attracted much attention as a promising therapy for the prevention of metastasis and relapse of malignant tumors, especially highly metastatic tumors such as melanoma. However, it is difficult to achieve a potent cancer vaccine effect by DNA vaccination, since the number of dendritic cells, which are the major targeted cells of DNA vaccination, is very few. Here, we developed a DNA vaccination for metastatic and relapsed melanoma by ultrasound (US)-responsive and antigen presenting cell (APC)-selective gene carriers reported previously, named Man-PEG_{2000} bubble lipoplexes. Following immunization using US exposure and Man-PEG_{2000} bubble lipoplexes constructed with pUb-M, which expresses ubiquitylated melanoma-specific antigens (gp100 and TRP-2), the secretion of Th1 cytokines (IFN-γ and TNF-α) and the activities of cytotoxic T lymphocytes (CTLs) were specifically enhanced in the presence of B16BL6 melanoma antigens. Moreover, we succeeded in obtaining potent and sustained DNA vaccine effects against solid and metastatic tumor derived from B16BL6 melanoma specifically. The findings obtained from this study suggest that the gene transfection method using Man-PEG_{2000} bubble lipoplexes and US exposure could be suitable for DNA vaccination aimed at the prevention of metastatic and relapsed cancer.

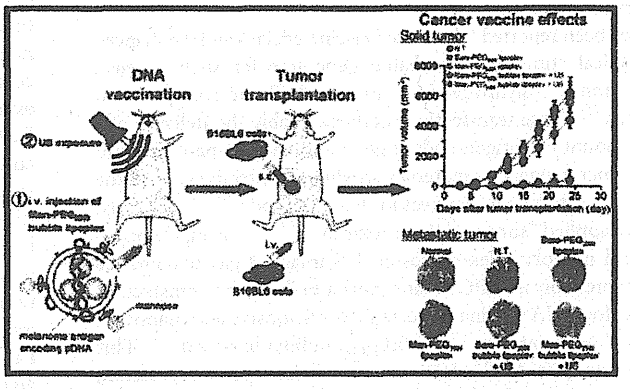

KEYWORDS: mannose modification, bubble lipoplex, ultrasound, DNA vaccination, melanoma

INTRODUCTION

Melanoma is a neoplasm arising within epidermal melanocytes of the skin, and one of several cancers exhibiting the increasing incidence in recent years.[1] Early stage melanoma is curable, but melanoma metastasis and relapse occur frequently in the patients following treatments such as surgery, and the prognosis for patients with metastatic melanoma is poor.[2,3] Although systemic therapy induces complete therapeutic responses in a minority of patients, metastatic melanoma is a devastating illness and treatment options are limited; therefore, there is a need for an effective therapy for metastatic melanoma.

Cancer vaccination has attracted much attention as a promising therapy for the prevention of tumor growth and metastasis, because it is based on an immune response provided by the cancer antigen, and consequently, its therapeutic effects are specific to the targeted cancer cells and the adverse effects followed by cancer vaccination are low.[4,5] In particular, it has been reported that DNA vaccination, which uses an exogenous gene encoding cancer antigen, can induce not only humoral immunity but also cellular immunity and, moreover, can induce cancer-specific CTLs with potent antitumor activities.[6−9] In a variety of cancers, since melanoma is known to exhibit inherent immunogenicity and the identification of melanoma-specific antigen is proceeding, such as gp100, melanoma-antigen recognized by T cells-1 (MART-1) and tyrosinase-related protein (TRP),[10−13] it is considered that DNA vaccination against melanoma is suitable for not only the

Received: October 29, 2010
Accepted: January 20, 2011
Revised: January 8, 2011
Published: January 20, 2011

prevention of metastasis and relapse but also the suppression of tumor growth.

To achieve potent therapeutic effects by DNA vaccination against cancer, it is essential to transfer the antigen-coding gene selectively and efficiently into APCs such as macrophages and dendritic cells, which play a pivotal role in the initiation, programming and regulation of cancer-specific immune responses.[14,15] Our group has also developed mannose-modified liposome/plasmid DNA (pDNA) complexes (mannose-modified lipoplexes) for APC-selective gene transfer via mannose receptors expressing on APCs, and obtained APC-selective gene expression in the liver and spleen by mannose-modified lipoplexes.[16,17] Moreover, our group also succeeded in obtaining DNA vaccine effects against cancer by intraperitoneal administration of mannose-modified lipoplexes constructed with tumor-specific antigen coding pDNA, such as ovalbumin (OVA) and melanoma-related antigens.[18,19] However, the gene transfection efficiency into APCs was lower than that in other cells;[20] therefore, it could be difficult to induce a potent cancer vaccine effect for the prevention of metastasis and relapse by DNA vaccination using conventional lipofection methods.

It has been reported that cancer vaccine effects can be enhanced by physical stimulation-mediated gene transfer such as electroporation,[21,22] hydrodynamic injection[23,24] and sonoporation methods.[25] These transfection methods enable the delivery of a large amount of antigen-coding gene and antigen peptides into APCs, since exogenous materials are directly introduced into the cytoplasm without endocytosis in these methods.[26−29] Recently, we have applied "sonoporation methods[25,29−31]" using US exposure and microbubbles enclosing US imaging gas to enhance gene expression in APCs[32] and developed a gene transfection method for DNA vaccination using US-responsive and mannose-modified gene carriers, Man-PEG_{2000} bubble lipoplexes.[33] This method enables APC-selective and -efficient gene expression, and moreover, effective vaccine effects against OVA-expressing cancer cells were obtained by applying this method to DNA vaccination using OVA-encoding pDNA.[33] However, the antigenicity of OVA is extremely high compared with other antigens,[34] and it is difficult to extrapolate the result obtained by DNA vaccination against OVA-expressing cells to actual cancer therapy, since OVA-expressing cells are transfectant constructed by gene transfer. Therefore, it is unclear if DNA vaccination by gene transfer using Man-PEG_{2000} bubble lipoplexes and US exposure is effective against cancer, i.e. melanoma, with metastatic properties.

In this study, we examined DNA vaccine effects against melanoma by transfection of pUb-M, coexpressing ubiquitylated gp100 and TRP-2, using Man-PEG_{2000} bubble lipoplexes and US exposure. First, we examined the level of gene expression in the splenic dendritic cells by gene transfer using Man-PEG_{2000} bubble lipoplexes constructed with pUb-M and US exposure. Second, we studied the characteristics of cytokine secretion and the induction of CTL activities against B16BL6 cell-derived melanoma by DNA vaccination using Man-PEG_{2000} bubble lipoplexes constructed with pUb-M and US exposure. Then, we investigated the cancer vaccine effects against solid and metastatic tumors derived from B16BL6 cells by DNA vaccination using Man-PEG_{2000} bubble lipoplexes and US exposure. Finally, we evaluated the duration of cancer vaccine effects against solid and metastatic melanoma after pUb-M transfection using Man-PEG_{2000} bubble lipoplexes and US exposure.

EXPERIMENTAL SECTION

Materials. 1,2-Stearoyl-3-trimethylammoniumpropane (DSTAP), 1,2-distearoyl-*sn*-glycero- 3-phosphocholine (DSPC) and 1,2-distearoyl-*sn*-glycero-3-phosphoethanolamine-*N*-[amino-(polyethylene glycol)-2000] (NH_2-PEG_{2000}-DSPE) were purchased from Avanti Polar Lipids Inc. (Alabaster, AL, USA), Sigma Chemicals Inc. (St. Louis, MO, USA) and NOF Co. (Tokyo, Japan), respectively. Anti-CD11c monoclonal antibody (N418)-labeled magnetic beads were obtained from Miltenyi Biotec Inc. (Auburn, CA, USA). Fetal bovine serum (FBS) was purchased from Equitech-bio Inc. (Kerrville, TX, USA). RPMI-1640 and Dulbecco's modified Eagle's medium (DMEM) were purchased from Nissui Pharmaceutical Co., Ltd. (Tokyo, Japan). All other chemicals were of the highest purity available.

pDNA, Cell Lines and Mice. pUb-M containing murine melanoma glycoprotein-100_{25-33} (gp100) and tyrosinase-related protein-$2_{181-188}$ (TRP-2) peptide epitopes was kindly provided by Prof. R. A. Reisfeld.[35] The B16BL6 melanoma cells, colon-26 adenocarcinoma cells and EL4 lymphoma cells were obtained from American Type Culture Collection (ATCC, Manassas, VA, USA). The B16BL6/Luc cells and colon-26/Luc cells, which are cell lines expressing firefly luciferase stably, were established as previously reported.[36,37] The B16BL6 cells and EL4 cells were cultured in DMEM, and the colon-26 cells were cultured in RPMI-1640 at 37 °C in 5% CO_2. Both media were supplemented with 10% FBS, 100 IU/mL penicillin, 100 μg/mL streptomycin, and 2 mM L-glutamine. Female C57BL/6 mice (6 weeks old) and female Balb/c mice (6 weeks old) were purchased from the Shizuoka Agricultural Cooperative Association for Laboratory Animals (Shizuoka, Japan). All animal experiments were carried out in accordance with the Principles of Laboratory Animal Care as adopted and propagated by the U.S. National Institutes of Health and the Guidelines for Animal Experiments of Kyoto University.

Construction of Man-PEG_{2000} Bubble Lipoplexes. Man-PEG_{2000} bubble lipoplexes were constructed according to our previous report.[33] Briefly, DSTAP, DSPC and NH_2-PEG_{2000}-DSPE or mannose-modified PEG_{2000}-DSPE were mixed in chloroform at a molar ratio of 7:2:1 to produce the liposomes for bubble lipoplexes. The mixture for construction of liposomes was dried by evaporation and vacuum desiccated, and the resultant lipid film was resuspended in sterile 5% dextrose. After hydration for 30 min at 65 °C, the dispersion was sonicated for 10 min in a bath sonicator and for 3 min in a tip sonicator to produce liposomes. Then, the liposomes were sterilized by passage through a 0.45 μm filter (Nihon-Millipore, Tokyo, Japan). The lipoplexes were prepared by gently mixing equal volumes of pDNA and liposome solution at a charge ratio of 1.0:2.3 (−:+). To enclose US imaging gas in lipoplexes, the prepared lipoplexes were pressured with perfluoropropane gas (Takachiho Chemical Industries Co., Ltd., Tokyo, Japan) and sonicated using a bath-type sonicator (AS ONE Co., Osaka, Japan) for 5 min. The particle sizes and zeta potentials of the liposomes/lipoplexes were determined by a Zetasizer Nano ZS instrument (Malvern Instrument, Ltd., Worcestershire, U.K.).

In Vivo Gene Transfection Method. Six week old C57BL/6 female mice were intravenously injected with 400 μL of bubble lipoplexes via the tail vein using a 26 gauge syringe needle at a dose of 50 μg of pDNA. At 5 min after the injection of the bubble lipoplexes, US (frequency, 1.045 MHz; duty, 50%; burst rate,

Table 1. Particle Sizes and Zeta Potentials of Lipoplexes and Bubble Lipoplexes Constructed with pUb-M[a]

	particle size (nm)	zeta-potential (mV)
Bare-PEG_{2000} lipoplex (DSTAP:DSPC:NH_2-PEG_{2000}-DSPE = 7:2:1 (mol))	144 ± 13	45.7 ± 4.5
Man-PEG_{2000} lipoplex (DSTAP:DSPC:Man-PEG_{2000}-DSPE = 7:2:1 (mol))	143 ± 10	44.5 ± 5.8
Bare-PEG_{2000} bubble lipoplex (DSTAP:DSPC:NH_2-PEG_{2000}-DSPE = 7:2:1 (mol))	557 ± 20	46.7 ± 4.2
Man-PEG_{2000} bubble lipoplex (DSTAP:DSPC:Man-PEG_{2000}-DSPE = 7:2:1 (mol))	555 ± 19	45.1 ± 2.2

[a] Each value represents the mean ± SD (n = 3).

10 Hz; intensity 1.0 W/cm^2; time, 2 min) was exposed transdermally to the abdominal area using a Sonopore-4000 sonicator with a probe of diameter 20 mm. At predetermined times after injection, mice were sacrificed and spleens were collected for each experiment. In the intradermal transfection study, mice were intradermally injected with 200 μL of bubble lipoplexes at a dose of 50 μg of pDNA. At 5 min after the injection of the bubble lipoplexes, US (frequency, 2.062 MHz; duty, 50%; burst rate, 10 Hz; intensity 4.0 W/cm^2; time, 2 min) was directly exposed to the injected site using a probe of diameter 6 mm. In the intrasplenic transfection, mice were directly injected into the spleen with 200 μL of bubble lipoplexes at a dose of 50 μg of pDNA. At 5 min after the injection of the bubble lipoplexes, US (frequency, 2.062 MHz; duty, 50%; burst rate, 10 Hz; intensity 4.0 W/cm^2; time, 2 min) was directly exposed to the spleen using a probe of diameter 6 mm.

Measurement of the Level of mRNA Expression. Total RNA was isolated from the spleen using a GenElute Mammalian Total RNA Miniprep Kit (Sigma-Aldrich, St. Louis, MO, USA). Reverse transcription of mRNA was carried out using a PrimeScript RT reagent Kit (Takara Bio Inc., Shiga, Japan). The detection of the Ub-M cDNA was carried out by real-time PCR using SYBR Premix Ex Taq (Takara Bio Inc., Shiga, Japan) and Lightcycler Quick System 350S (Roche Diagnostics, Indianapolis, IN, USA) with primers. The primers for Ub-M, gp100, TRP-2 and GAPDH cDNA were constructed as follows: primer for Ub-M cDNA, 5′-GAG CCC AGT GAC ACC ATA GA-3′ (forward) and 5′-GTG CAG GGT GGA CTC TTT CT-3′ (reverse); primer for gp100, 5′-GCA CCC AAC TTG TTG TTC CT-3′ (forward) and 5′-GTG CTA CCA TGT GGC ATT TG-3′ (reverse); primer for TRP-2, 5′-CTT CCT AAC CGC AGA GCA AC-3′ (forward) and 5′-CAG GTA GGA GCA TGC TAG GC-3′ (reverse); primer for GAPDH, 5′-TCT CCT GCG ACT TCA ACA-3′ (forward) and 5′-GCT GTA GCC GTA TTC ATT GT-3′ (reverse) (Sigma-Aldrich, St. Louis, MO, USA). The mRNA copy numbers were calculated for each sample from the standard curve using the instrument software ("Arithmetic Fit Point analysis" for the Lightcycler). Results were expressed as relative copy numbers calculated relative to GAPDH mRNA (copy numbers of Ub-M, gp100 and TRP-2 mRNA/copy numbers of GAPDH mRNA).

Isolation of Splenic $CD11c^+$ Cells (Dendritic Cells) in Mice. At 6 h after transfection, spleens were harvested and spleen cells were suspended in ice-cold RPMI-1640 medium on ice. Then, red blood cells were removed by incubation with hemolytic reagent (0.15 M NH_4Cl, 10 mM $KHCO_3$, 0.1 mM EDTA) for 3 min at room temperature. $CD11c^+$ and $CD11c^-$ cells were separated by magnetic cell sorting with an auto MACS (Miltenyi Biotec Inc., Auburn, CA, USA) following the manufacturer's instructions.

Evaluation of Antigen-Specific Cytokine Secretion. To prepare the tumor cell lysates (B16BL6 cells, EL4 cells and colon-26 cells), the cells were scraped from the plates and suspended in lysis buffer (0.05% Triton X-100, 2 mM EDTA, 0.1 M Tris, pH 7.8). After three cycles of freezing and thawing, the lysates were centrifuged at 10000g, 4 °C for 10 min and the resultant supernatants were collected. The protein concentration of cell lysates was determined with a Protein Quantification Kit (Dojindo Molecular Technologies, Inc., Tokyo, Japan). At 2 weeks after the last immunization, the splenic cells collected from immunized mice were plated in 96-well plates and incubated for 72 h at 37 °C in the presence or absence of tumor cell lysates (100 μg of proteins). IFN-γ, TNF-α, IL-4 and IL-6 in the culture medium were measured using a suitable commercial ELISA Kit (Bay Bioscience Co., Ltd., Hyogo, Japan).

CTL Assay. At 2 weeks after the last immunization, the splenic cells collected from immunized mice were plated in 6-well plates and coincubated with mitomycin C-treated tumor cells (B16BL6 cells, EL4 cells and colon-26 cells) for 4 days. After 4 days of coincubation, nonadherent cells were harvested, washed and plated in 96-well plates with target cells (B16BL6 cells, EL4 cells and colon-26 cells) at various effector cell/target cell (E/T) ratios. The target tumor cells were labeled with ^{51}Cr by incubating with $Na_2{}^{51}CrO_4$ (PerkinElmer, Inc., MA, USA) in culture medium for 1 h at 37 °C. At 4 h after incubation, the plates were centrifuged, and the supernatant in each well was collected and the radioactivity of released ^{51}Cr was measured in a gamma counter. The percentage of ^{51}Cr release was calculated as follows: specific lysis (%) = [(experimental ^{51}Cr release − spontaneous ^{51}Cr release)/(maximum ^{51}Cr release − spontaneous ^{51}Cr release)] × 100).

Therapeutic Experiments in Solid Tumor Models. At 2 weeks after the last immunization or on the immunization day, B16BL6 cells, EL4 cells and colon-26 cells were transplanted subcutaneously into the back of the mice (1×10^6 cells). The tumor size was measured with calipers in two dimensions, and the tumor volume was calculated using the following equation: volume (mm^3) = $\pi/6 \times$ longer diameter × (shorter diameter)^2. The survival of the mice was monitored up to 100 days after the transplantation of tumor cells.

Therapeutic Experiments in Lung Metastatic Tumor Models. At 2 weeks after the last immunization or on the immunization day, B16BL6 cells or colon-26 cells were intravenously administered via the tail vein (1×10^5 cells) and the survival of the mice was monitored up to 100 days after administration of the tumor cells. To evaluate metastasis, B16BL6/Luc cells or colon-26/Luc cells were intravenously administered via the tail vein (1×10^5 cells). At 14 days after the administration of the tumor cells, the number of B16BL6/Luc cells and colon-26/Luc cells in the lung was quantitatively evaluated by measuring luciferase activity as previously reported.[36,37]

Statistical Analysis. Results were presented as the mean ± SD of more than three experiments. Analysis of variance (ANOVA) was used to test the statistical significance of differences among groups. Two-group comparisons were performed by the Student's t test. Multiple comparisons between control groups and other groups were performed by the Dunnett's test, and multiple

comparisons between all groups were performed by the Tukey–Kramer test.

RESULTS

Physicochemical Properties of Bubble Lipoplexes Constructed with pUb-M. The physicochemical properties of lipoplexes and bubble lipoplexes constructed with pUb-M used in all experiments were evaluated by measuring the particle sizes and zeta potentials. The mean particle sizes and zeta potentials of nonmodified PEG_{2000}-lipoplexes (Bare-PEG_{2000} lipoplexes) and mannose-conjugated PEG_{2000}-lipoplexes (Man-PEG_{2000} lipoplexes) were 144 ± 13 nm, 45.7 ± 4.5 mV and 143 ± 10 nm, 44.5 ± 5.8 mV, respectively (Table 1). Moreover, the mean particle sizes and zeta potentials of nonmodified bubble lipoplexes (Bare-PEG_{2000} bubble lipoplexes) and Man-PEG_{2000} bubble lipoplexes were 557 ± 20 nm, 46.7 ± 4.2 mV and 555 ± 19 nm, 45.1 ± 2.2 mV, respectively (Table 1). These results corresponded to our previous reports using other pDNA,[33] suggesting that pDNA had no effect on the physicochemical properties of Man-PEG_{2000} bubble lipoplexes.

Splenic Dendritic Cell-Selective and -Efficient Gene Expression by Gene Transfer Using Man-PEG_{2000} Bubble Lipoplexes and US Exposure. First, to investigate the level of gene expression by Man-PEG_{2000} bubble lipoplexes and US exposure in the spleen, we measured the relative mRNA copy numbers of Ub-M after transfection. As shown in Figures 1A and 1B, the level of Ub-M mRNA expression obtained by Man-PEG_{2000} bubble lipoplexes and US exposure reached a peak at 6 h after transfection. Moreover, that level of Ub-M mRNA expression was markedly higher than that obtained by Bare- and Man-PEG_{2000} lipoplexes, and significantly higher than that obtained by Bare-PEG_{2000} bubble lipoplexes and US exposure. Then, we investigated the mannose receptor-expressing cell selectivity of Ub-M mRNA expression obtained by gene transfer using Man-PEG_{2000} bubble lipoplexes and US exposure. In the spleen, the relative mRNA copy numbers of Ub-M in $CD11c^+$ cells was significantly higher than that in $CD11c^-$ cells following transfection using Man-PEG_{2000} bubble lipoplexes and US exposure (Figure 1C). On the other hand, no selective gene expression in $CD11c^+$ cells was observed by gene transfer using Bare-PEG_{2000} bubble lipoplexes and US exposure (Figure 1C).

Antigen-Stimulatory Th1 Cytokine Secretion from the Splenic Cells Immunized by Man-PEG_{2000} Bubble Lipoplexes and US Exposure. To evaluate the melanoma-specific cytokine secretion from immunized splenic cells, splenic cells immunized by pUb-M were incubated with each tumor cell-lysate in vitro, and then, Th1 and Th2 cytokines secreted in the supernatants were measured. Following investigation of the expression level of gp100 and TRP-2, a melanoma-specific antigen, in each cell used in this study, the expression of gp100 and TRP-2 was only detected in B16BL6 cells which are melanoma cell lines (Supplementary Figure 1 in the Supporting Information). As results of the immunization according to the protocol shown in Figure 2A, the splenic cells immunized by Man-PEG_{2000} bubble lipoplexes and US exposure secreted the highest amount of IFN-γ and TNF-α, which are Th1 cytokines, in the presence of B16BL6 cell lysates (Figures 2B and 2C). On the other hand, the secretion of Th1 cytokines (IFN-γ and TNF-α) was lower in all the groups in the presence of EL4 and colon-26 cell lysates. Moreover, the secretion of IL-4 and IL-6, which are Th2 cytokines, was also lower in all the groups in the presence of each cell lysate (Figures 2D and 2E). These observations suggest that pUb-M transfer by Man-PEG_{2000} bubble lipoplexes and US exposure significantly enhances the differentiation of helper T cells into Th1.

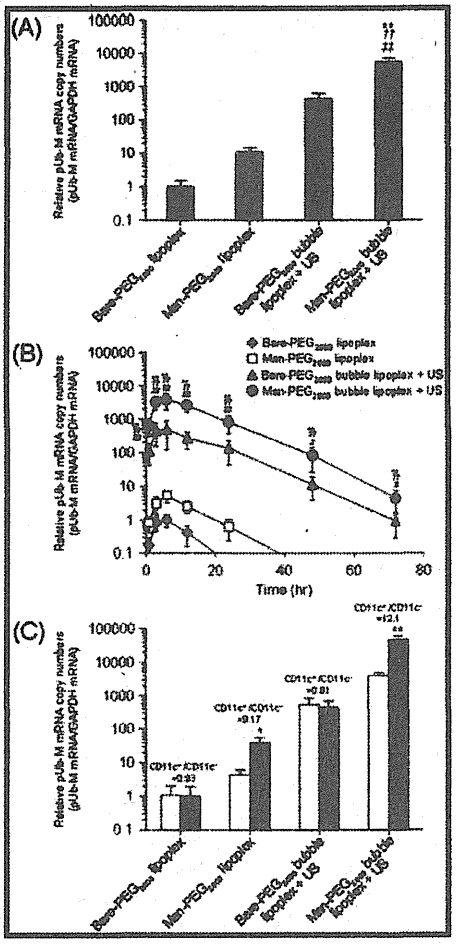

Figure 1. Enhanced Ub-M mRNA expression in the spleen and the splenic dendritic cells ($CD11c^+$ cells) by Man-PEG_{2000} bubble lipoplexes constructed with pUb-M and US exposure in vivo. (A) The level of Ub-M mRNA expression obtained by Bare-PEG_{2000} lipoplexes, Man-PEG_{2000} lipoplexes, Bare-PEG_{2000} bubble lipoplexes with US exposure and Man-PEG_{2000} bubble lipoplexes with US exposure (50 μg of pDNA) in the spleen at 6 h after transfection. Each value represents the mean + SD (n = 4). $^{**}p < 0.01$, compared with Bare-PEG_{2000} lipoplex; $^{\dagger\dagger}p < 0.01$, compared with Man-$PEG_{2000}$ lipoplex; $^{\ddagger\ddagger}p < 0.01$, compared with Bare-$PEG_{2000}$ bubble lipoplex + US. (B) Time-course of Ub-M mRNA expression in the spleen after transfection by Bare-PEG_{2000} lipoplexes, Man-PEG_{2000} lipoplexes, Bare-PEG_{2000} bubble lipoplexes with US exposure and Man-PEG_{2000} bubble lipoplexes with US exposure (50 μg of pDNA). Each value represents the mean ± SD (n = 4). $^{**}p < 0.01$, compared with the corresponding group of Bare-PEG_{2000} lipoplex; $^{\dagger\dagger}p < 0.01$, compared with the corresponding group of Man-PEG_{2000} lipoplex; $^{\ddagger}p < 0.05$; $^{\ddagger\ddagger}p < 0.01$, compared with the corresponding group of Bare-PEG_{2000} bubble lipoplex + US. (C) Splenic cellular localization of Ub-M mRNA expression at 6 h after transfection by Bare-PEG_{2000} lipoplexes, Man-PEG_{2000} lipoplexes, Bare-PEG_{2000} bubble lipoplexes with US exposure and Man-PEG_{2000} bubble lipoplexes with US exposure (50 μg of pDNA). Each value represents the mean + SD (n = 4). $^{*}p < 0.05$; $^{**}p < 0.01$, compared with the corresponding group of $CD11c^-$ cells.

Induction of Melanoma-Specific CTLs by pUb-M Transfer Using Man-PEG_{2000} Bubble Lipoplexes and US Exposure. We investigated the melanoma-specific CTL activities in the

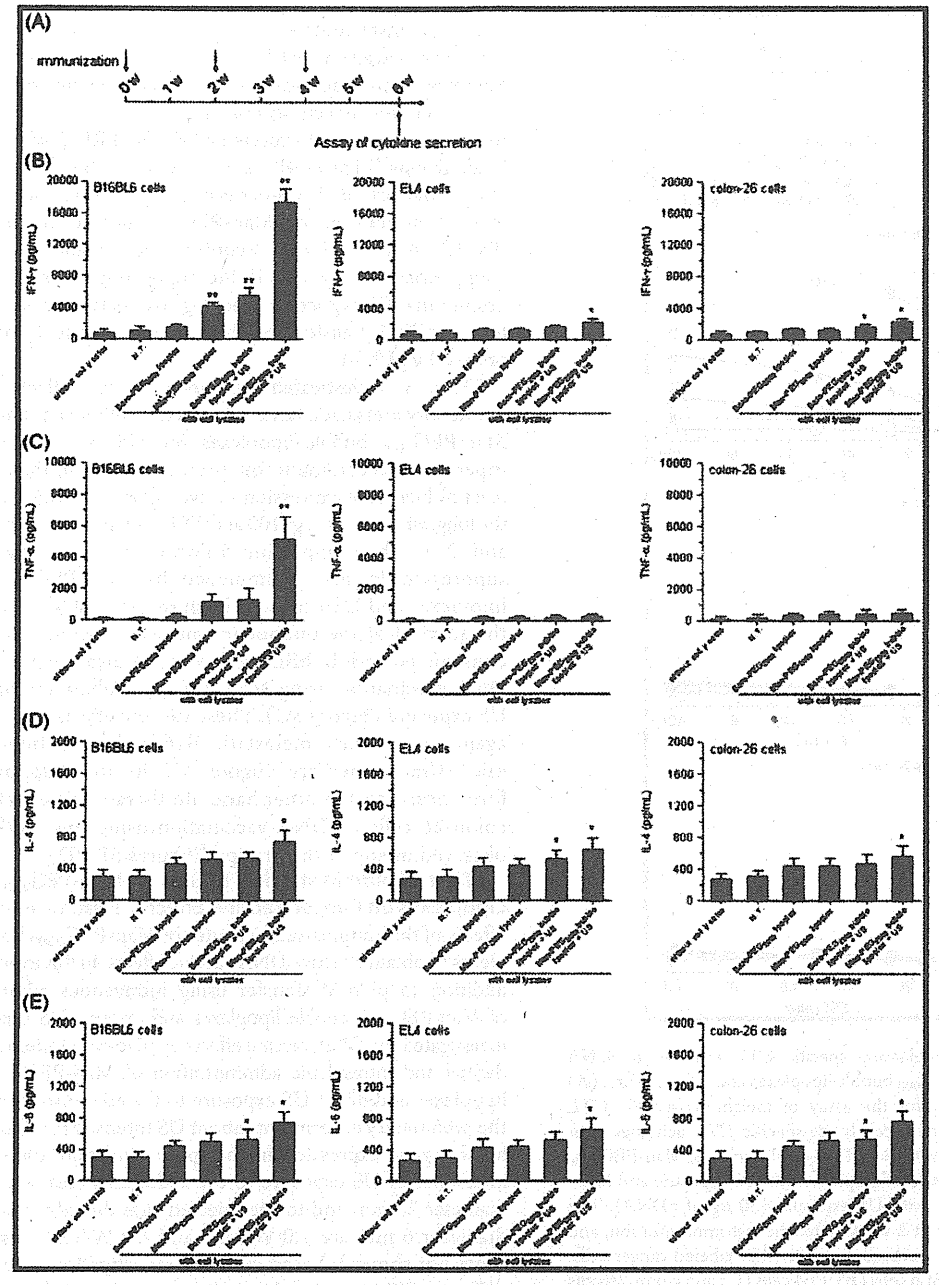

Figure 2. Melanoma-stimulatory cytokine secretion characteristics by DNA vaccination using Man-PEG_{2000} bubble lipoplexes constructed with pUb-M and US exposure. (A) Schedule of immunization for the evaluation of melanoma-stimulatory cytokine secretion characteristics. (B−E) Each cancer cell lysate-specific IFN-γ (B), TNF-α (C), IL-4 (D) and IL-6 (E) secretion from the splenic cells immunized three times biweekly with Bare-PEG_{2000} lipoplexes, Man-PEG_{2000} lipoplexes, Bare-PEG_{2000} bubble lipoplexes with US exposure and Man-PEG_{2000} bubble lipoplexes with US exposure (50 μg of pDNA). The splenic cells were collected at 2 weeks after the last immunization. After the immunized splenic cells were cultured for 72 h in the presence of each cancer cell lysate (100 μg protein), IFN-γ, TNF-α, IL-4 and IL-6 secreted in the medium were measured by ELISA. Each value represents the mean + SD ($n = 4$). $^*p < 0.05$; $^{**}p < 0.01$, compared with the corresponding "without cell lysate" group.

splenic cells immunized by pUb-M. This experiment was performed according to the protocol shown in Figure 3A. As shown in Figure 3B, the splenic cells immunized by Man-PEG_{2000} bubble lipoplexes and US exposure showed the highest CTL activities of all groups stimulated by B16BL6 cells. In contrast, no CTL activity was obtained in all groups stimulated by EL4 and colon-26 cells (Figures 3C and 3D). These results suggest that melanoma-specific CTLs are induced effectively in the splenic cells transfected pUb-M by Man-PEG_{2000} bubble lipoplexes and US exposure.

Cancer Vaccine Effects against Melanoma-Derived Solid and Metastatic Tumors by DNA Vaccination Using Man-PEG_{2000} Bubble Lipoplexes and US Exposure. Cancer vaccine effects against solid and metastatic tumors obtained by DNA vaccination using Man-PEG_{2000} lipoplexes and US exposure were examined. First, we evaluated the level of gp100 and